

**THE EFFECT OF GLIBENCLAMIDE IN
LIPOPOLYSACCHARIDE STIMULATED BRAIN
MICROVASCULAR ENDOTHELIAL CELLS**

**A Thesis Submitted to
the Graduate School of Engineering and Science of
İzmir Institute of Technology
in Partial Fulfillment of the Requirements for the Degree of**

MASTER OF SCIENCE

in Molecular Biology and Genetics

**by
Hilal CİHANKAYA**

**July 2019
İZMİR**


We approve the thesis of **Hilal CİHANKAYA**

Examining Committee Members:



Assist. Prof. Dr. Çiğdem TOSUN

Department of Molecular Biology and Genetics, İzmir Institute of Technology



Assoc. Prof. Dr. Gülistan MEŞE ÖZÇİVİCİ

Department of Molecular Biology and Genetics, İzmir Institute of Technology



Assoc. Prof. Dr. Duygu SAĞ WİNGENDER

Department of Medical Biology, Faculty of Medicine, Dokuz Eylül University

11 July 2019



Assist. Prof. Dr. Çiğdem TOSUN

Supervisor, Department of Molecular Biology and Genetics, İzmir Institute of Technology



Prof. Dr. Volkan SEYRANTEPE

Head of the Department of Molecular Biology and Genetics

Prof. Dr. Aysun SOFUOĞLU

Dean of the Graduate School of Engineering and Sciences

ACKNOWLEDGMENTS

I would like to express my sincere thanks and appreciation to my supervisor Assist. Prof. Dr. ıgdem TOSUN who has guided me throughout my master's thesis and shared her scientific knowledge and experience with me. I have been exceptionally lucky to have a supervisor like her and I am very grateful for her kindness, continuous support, encouragement and optimism.

I deeply appreciate and thank to Assoc. Prof. Dr. Alper ARSLANOĐLU who generously opened his laboratory to me for the cell culture experiments, Assoc. Prof. Dr. Duygu SAĐ WİNGENDER who kindly provided LPS for this study and Assoc. Prof. Dr. Glistan MEŐE ZĐİVİCİ who gave me the opportunity to use fluorescent microscope and Prof. Dr. Hseyin ađlar KARAKAYA who opened his laboratory to me, as well.

I also would like to thank my friends Bora TAŐTAN, İsmail TAHMAZ and Yađmur Ceren NAL for their unquestionable support and contributions especially during the troubleshooting of some experiments. It would be hardly possible to finish this journey without their motivation and help.

I would like to thank my mother Zekiye CİHANKAYA, my father Hayati CİHANKAYA and my sister Őevval CİHANKAYA for their timeless support and help. They have never stopped believing in me and motivated me throughout my life.

At last but not least, I would like to express my gratitude to H. Gkberk ZĐELİK who has kept me motivated during my master's thesis with all its ups and downs. I would like to thank him for his constant patience, support and endless love.

ABSTRACT

THE EFFECT OF GLIBENCLAMIDE IN LIPOPOLYSACCHARIDE STIMULATED BRAIN MICROVASCULAR ENDOTHELIAL CELLS

Endothelial cells are essential components of the blood brain barrier (BBB) that regulate the exchange of solutes between the vasculature and the brain parenchyma. The integrity of the BBB is disrupted after central nervous system (CNS) injuries, and it has been associated with the Sur1-Trpm4 channels. Once these channels are opened, Na⁺ flows into the cells causing edema and cell death. To mimic CNS injuries *in vitro*, lipopolysaccharide (LPS) was used as an endotoxin to initiate proinflammatory mediators to increase endothelial permeability, and glibenclamide was used as an antagonist of Sur1-Trpm4 channels to reduce the inflammatory response and to maintain the structural integrity of BBB proteins. To demonstrate the role of glibenclamide following LPS stimulation, we determined the cytotoxicity of LPS in bEnd.3 cells by cleaved caspase-3 expression and propidium iodide staining. We also investigated the protective effect of glibenclamide on NF-κB translocation, and BBB proteins; collagen IV (COL IV) and zonula occludens 1 (ZO-1) in LPS stimulated bEnd.3 cells. Our results revealed that 1μg/ml LPS exposure was sufficient for NF-κB nuclear translocation, along with a statistically significant decrease in the expressions of COL IV and ZO-1 proteins, and a significant increase in cell death. We also demonstrated that glibenclamide was able to restore the expressions of COL IV and ZO-1, significantly reduce NF-κB translocation, and cell death. Taken together, LPS induction in bEnd.3 cells can be used to investigate endothelial cell dysfunction due to inflammation in stroke and trauma models and glibenclamide can be used as a protective drug to inhibit LPS stimulated inflammatory response, cell death and disruptions in the structures of key BBB proteins.

Keywords: brain microvascular endothelial cells, lipopolysaccharide, glibenclamide, Sur1-Trpm4 channel

ÖZET

GLİBENKLAMİDİN LİPOLİSAKKARİT İLE UYARILMIŞ BEYİN MİKROVASKÜLER ENDOTEL HÜCRELERİNDEKİ ETKİSİ

Endotel hücreleri, beyin parankiması ve vaskülatür arasında maddelerin değişimini düzenleyen kan beyin bariyerinin (BBB) temel bileşenleridir. BBB bütünlüğü, merkezi sinir sistemi (MSS) yaralanmalarının ardından bozulur ve bu Sur1-Trpm4 kanalları ile ilişkilendirilmiştir. Bu kanallar açıldığında, Na⁺ hücre içine geçerek, ödem ve hücre ölümüne neden olur. Bu çalışmada *in vitro* MSS yaralanmalarını taklit etmek için bir endotoksin olarak lipopolisakarit (LPS) endotel geçirgenliğini arttıran proinflamatuvar mediatörlerin ifadelerini başlatmak için ve glibenklamid bu inflamatuvar tepkileri azaltmak ve BBB'nin yapısal bütünlüğünü korumak için Sur1-Trpm4 kanallarının bir antagonisti olarak kullanıldı. LPS stimülasyonunu takiben, bEnd.3 hücrelerinde glibenklamidin rolünü göstermek için, LPS sitotoksitesini aktive olmuş kaspaz-3 ekspresyonu ve propidium iyodür boyaması ile belirledik. Ayrıca glibenklamidin LPS ile uyarılmış bEnd.3 hücrelerindeki koruyucu etkisini NF-κB translokasyonu ve BBB proteinleri olan kollajen IV (COL IV) ve zonula okludens 1 (ZO-1) üzerinde araştırdık. Sonuçlarımız, 1 µg / ml LPS'ye maruz kalmanın NF-κB nükleer translokasyonu için yeterli olduğunu, COL IV ve ZO-1 proteinlerinin ifadelerinde istatistiksel olarak anlamlı bir düşüş ve hücre ölümünde anlamlı bir artış olduğunu ortaya koydu. Ayrıca, glibenklamidin COL IV ve ZO-1 ekspresyonlarını geri getirebildiğini, NF-κB translokasyonunu ve hücre ölümünü anlamlı olarak azalttığını gösterdik. Birlikte ele alındığında, bEnd.3 hücrelerinde LPS indüksiyonu, inme ve travma modellerinde iltihaplanma nedeniyle endotel hücre disfonksiyonunu araştırmak için kullanılabilir ve glibenklamid, LPS ile uyarılan iltihaplanma tepkilerini, hücre ölümünü ve temel BBB proteinlerinin yapılarındaki bozulmaları engellemek için koruyucu bir ilaç olarak kullanılabilir.

Anahtar Kelimeler: beyin mikrovasküler endotel hücreleri, lipopolisakarit, glibenklamid, Sur1-Trpm4 kanalları

TABLE OF CONTENTS

LIST OF TABLES	viii
LIST OF FIGURES	ix
LIST OF ABBREVIATIONS.....	x
CHAPTER 1 INTRODUCTION	1
1.1. Brain Microvascular Endothelial Cells.....	1
1.2. Sulfonyl Urea Receptor 1	2
1.2.1. Sur1-K _{ir} 6.2 Channels.....	3
1.2.2. Sur1-Trmp4 Channels	3
1.3. Glibenclamide	6
1.4. TLR4 Signaling.....	7
1.4.1. TLR4 Activation.....	8
1.4.2. Myd88 Dependent Signaling.....	9
1.4.3. Myd88 Independent Pathway	9
1.5. Aim and Hypothesis.....	10
CHAPTER 2 MATERIALS AND METHODS	11
2.1 Materials	11
2.2 Methods	11
2.2.1 Cell Culture	11
2.2.2 Subculturing	11
2.2.3 Cell Freezing and Thawing	12
2.2.4 Propidium Iodide and Hoechst Staining.....	13
2.2.5 Protein Isolation.....	13
2.2.6 Determination of Protein Concentration by BCA	14
2.2.7 Western Blotting.....	15
2.2.8 Immunostaining.....	16

2.2.9 Image Analysis with ImageJ	18
2.2.10 Statistical Analysis	20
CHAPTER 3 RESULTS	21
3.1 Investigation of Cell Death via Cleaved Caspase-3 Expression in LPS Stimulated bEnd.3 cells	21
3.2 Determination of Cell Death via Propidium Iodide and Hoechst Staining	23
3.3 The Effect of Glibenclamide on NFκB Translocation.....	23
3.4 The Effect of Glibenclamide on Collagen IV in LPS Stimulated bEnd.3 Cells.....	26
3.5 The Effect of Glibenclamide on Zonula Occludens-1 in LPS Stimulated bEnd.3 cells	26
CHAPTER 4 DISCUSSION.....	30
CHAPTER 5 CONCLUSION	34
REFERENCES	35

LIST OF TABLES

<u>Table</u>	<u>Page</u>
Table 2.1. The seeding numbers of cells in different types of culture plates.	12
Table 2.2. 2X RIPA buffer recipe	14
Table 2.3. Separating gel recipe for different percentages (For 10 ml).....	16
Table 2.4. Stacking gel recipe.....	17
Table 2.5. 4X Resolving buffer (For 200 ml).....	17
Table 2.6. 4X Stacking buffer (For 200 ml)	17
Table 2.7. 10X Running buffer recipe (For 500 ml).....	17
Table 2.8. 1X Transfer buffer recipe (For 500 ml).....	18
Table 2.9. 1X TBS-0.1% Tween-20 recipe (For 500 ml)	18
Table 2.10. Primary antibody list (IF: Immunofluorescence, WB: Western blotting) ...	18
Table 2.11. Secondary antibody list.....	18

LIST OF FIGURES

<u>Figure</u>	<u>Page</u>
Figure 1.1. Representations of the Sur1- K _{ir} 6.2 and the Sur1-Trpm4 channels	2
Figure 1.2. Representations of cytotoxic, ionic and vasogenic edema leading to hemorrhagic transformation.....	5
Figure 1.3. LPS activates TLR4 signaling in Myd88 dependent and independent pathways	8
Figure 2.1 Image analysis of NFκB on ImageJ	19
Figure 2.2. Image analysis of Hoechst stained images via ImageJ.....	20
Figure 3.1 Cleaved caspase-3 is upregulated in bEnd.3 cells after LPS stimulation.....	22
Figure 3.2. The effect of glibenclamide on cell death in LPS stimulated bEnd.3 cells	24
Figure 3.3. Glibenclamide reduces the amount of NFκB translocation into the nucleus in 24 hours LPS stimulated bEnd.3 cells.....	25
Figure 3.4. Glibenclamide reduces the amount of NFκB translocation into the nucleus in 48 hours LPS stimulated bEnd.3 cells	25
Figure 3.5. Glibenclamide interferes with collagen IV in 24 hours LPS stimulated bEnd.3 cells.....	27
Figure 3.6. Glibenclamide increases the amount of collagen IV in 48 hours LPS stimulated bEnd.3 cells	27
Figure 3.7. Glibenclamide restores the tight junction protein, zonula occludens-1 in 24 hours LPS stimulated bEnd.3 cells	28
Figure 3.8. Glibenclamide restores the tight junction protein, zonula occludens-1 in 48 hour LPS stimulated bEnd.3 cells.....	28

LIST OF ABBREVIATIONS

ABC	ATP binding cassette
AJ	Adherent junction
ANOVA	Analysis of variance
AP1	Activator protein 1
ATP	Adenosine triphosphate
BBB	Blood brain barrier
bEnd.3	Brain microvascular endothelial cell line
CD14	Cluster of differentiation 14
CNS	Central nervous system
COL IV	Collagen type IV
DAMP	Danger associated molecular pattern
DAPI	4',6-diamino-2-phenylindole
DD	Death domain
DM2	Diabetes mellitus type 2
DMSO	Dimethyl sulfoxide
DPBS	Dulbecco's phosphate buffered saline
ECL	Enhanced chemiluminescence
ECM	Extracellular matrix
EDTA	Ethylenediaminetetraacetic acid
FADD	Fas associated death domain
FBS	Fetal bovine serum
HRP	Horseradish peroxidase
ICH	Intracerebral hemorrhage
IFN	Interferon
I κ B	Inhibitor of NF- κ B
IKK	I κ B kinase
IL	Interleukin
IRAK	Interleukin 1 receptor associated kinase
IRF3	Interferon regulatory factor 3
K _{ATP}	ATP sensitive potassium channel
KO	Knock out
LBP	LPS binding protein
LPS	Lipopolysaccharide
LPS+Glib	Glibenclamide treated and LPS stimulated cells
MAPK	Mitogen activated protein kinase
MD2	Myeloid differentiation factor 2
MMP	Matrix metalloproteinase
Myd88	Myeloid differentiation factor 88
NCT	National clinical trial
NF- κ B	Nuclear factor kappa b
NOS	Nitrogen oxide species
PAMP	Pathogen associated molecular pattern
PBS	Phosphate buffered saline
PECAM1	Platelet endothelial cellular adhesion molecule 1
PI	Propidium iodide
PI3K	Phosphoinositide 3-kinase

PRR	Pattern recognition receptor
RIPA	Radioimmunoprecipitation assay buffer
ROI	Region of interest
ROS	Reactive oxygen species
SAH	Subarachnoid hemorrhage
SCI	Spinal cord injury
SDS	Sodium dodecyl sulfate
SDS PAGE	SDS polyacrylamide gel electrophoresis
SEM	Standard error of mean
SFM	Serum free medium
Sur1	Sulfonyl urea receptor 1
TBI	Traumatic brain injury
TBS	Tris buffered saline
TIR	Toll/interleukin 1 receptor
TIRAP	TIR domain containing adaptor protein
TJ	Tight junction
TLR4	Toll like receptor 4
TNF α	Tumor necrosis factor alpha
TNFR1	TNF α receptor 1
TRAF	TNF receptor associated factor
TRAM	TRIF related adaptor molecule
TRIF	Toll/IL1 receptor containing adaptor inducing IFN β
Trpm4	Transient receptor potential melastatin 4
ZO	Zonula occludens

CHAPTER 1

INTRODUCTION

1.1. Brain Microvascular Endothelial Cells

Blood brain barrier (BBB) separates the cerebral vasculature from the brain parenchyma, protects the brain from toxic chemicals and supplies O₂ and glucose to the brain ^[1]. BBB is mainly composed of endothelial cells and additional cells including astrocytic end feet, neurons, pericytes and the basement membrane proteins are critical for its integrity and proper functioning. Any problem with the vasculature or the structural integrity of the BBB will directly affect the brain and have devastating consequences.

Brain vascular endothelial cells are found in the innermost layer of the BBB and they interact directly with blood. They are connected to each other via tight junctions (TJs) and adherent junctions (AJs) ^[2]. TJs are mainly composed of claudin and occludin, which form dimers with each other between adjacent endothelial cells. Furthermore, junctional adhesion proteins can be found on TJs which can interact with platelet endothelial cellular adhesion molecule 1 (PECAM1) to take part in the leukocyte migration ^[3]. TJs are connected to the cytoskeletal actin via some accessory proteins namely, zonula occludens (ZO) 1, 2 and 3, which provide structural support to these cells ^[3]. Cadherin and catenin are the main molecules of AJs, which help the formation of TJs and give additional support to them. Any disruption in the structure of these junctional proteins have been linked to the increased permeability of the BBB, and has been reported in hypoxia/ischemia, brain trauma, encephalitis, meningitis, multiple sclerosis, Alzheimer's and Parkinson's diseases ^[4-9].

Pericytes interact with endothelial cells through gap junctions and support the endothelium in cerebral blood flow, cell proliferation, cell survival and migration ^[1, 10]. Together with endothelial cells, pericytes are also surrounded by the vascular basal lamina which is composed of extracellular matrix (ECM) proteins such as laminin, collagen type IV (COL IV), heparin sulphate proteoglycan and fibronectin ^[11]. All of these ECM proteins in the vascular basal lamina act as an anchor and a protective barrier for the cerebral endothelium, which are also responsible for the maintenance of TJ

proteins [11]. The weakened integrity of the vascular basal lamina proteins has been associated with an increased permeability of the BBB due to the elevated activity of matrix metalloproteinase (MMP) 2 and 9 [12]. MMPs are able to degrade the basal lamina and TJ proteins, causing BBB disruption and lead to vasogenic edema in stroke patients [13]. In addition, MMP 9 knock out (KO) mice and MMP 9 inhibitors have been shown to be protective at both the histological and functional level in adult ischemic and hemorrhagic stroke models by preventing further secondary damage through hemorrhagic transformation [14-16]. The basal lamina is also in direct contact with astrocytic end feet and their interaction further stabilize the function, tightness and development of BBB [1]. Astrocytes are glial cells that surround the brain parenchyma, maintain BBB integrity and link cerebral endothelial cells to the neurons [2]. All these interactions within the members of the BBB are crucial for its proper functioning.

1.2. Sulfonyl Urea Receptor 1

Sulfonyl urea receptor 1 (Sur1) is a transmembrane protein, which is in the family of the ATP binding cassette (ABC) transporters [17]. As an exception to the ABC transporters, Sur1 interacts with the heterologous pore forming subunits in order to form a functional ion channel, instead of transporting molecules via ATP hydrolysis. As a regulatory subunit, Sur1 can couple with either Kir6.2 or Trpm4 subunits to create different heteromultimeric ion channels (Figure 1.1). Even though both of these channels are activated by ATP depletion, they demonstrate different characteristics.

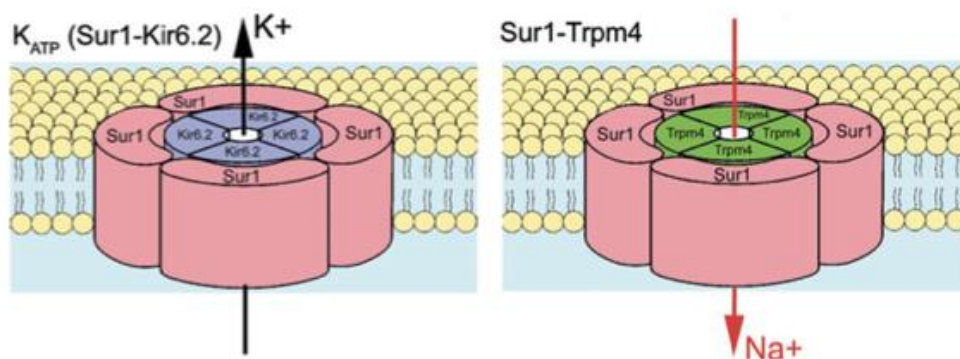


Figure 1.1. Representations of the Sur1- Kir6.2 and the Sur1-Trpm4 channels. Both channels have heterooctameric structures, which are composed of four regulatory Sur1 subunits and either four Kir6.2 or four Trpm4 subunits to form Sur1- Kir6.2 and Sur1-Trpm4 channels, respectively. The Sur1- Kir6.2 channel is responsible for K⁺ efflux, which causes hyperpolarization, whereas the Sur1-Trpm4 channel is responsible for Na⁺ influx, which causes depolarization of the cell. (Simard *et al.* [18])

1.2.1. Sur1-K_{ir}6.2 Channels

Sur1 couples with K_{ir}6.2 to form ATP sensitive K⁺ (K_{ATP}) channels, which are responsible for K⁺ efflux, hyperpolarization and insulin release in pancreatic β cells. In healthy cells, the ATP/ADP ratio is elevated upon glucose uptake, which results in the closure of Sur1- K_{ir}6.2 channels. This leads to an increased concentration of intracellular K⁺ and depolarizes the cell. Depolarization triggers the opening of voltage sensitive calcium channels and in turn causes an increase in the intracellular calcium levels, which ultimately causes the secretion of insulin via exocytosis in the pancreatic β cells [19]. On the other hand, unhealthy cells with diabetes mellitus type 2 (DM 2) is described by their resistance to insulin, which leads to less glucose uptake and insulin secretion [20]. Using Sur1 inhibitors as a treatment for DM 2 ensures the closure of Sur1- K_{ir}6.2 channels and provides insulin secretion [21].

In addition to their roles in pancreatic cells, Sur1- K_{ir}6.2 channels have been shown to be expressed in the CNS as well. A study by Castro *et al.*, revealed the expression of K_{ir}6.2 in neurons, microglia and astrocytes, however, the K_{ir}6.2 subunit was reported to only be significantly upregulated in astrocytes in tissues from traumatic brain injury (TBI) patients [22]. Similarly, Ortega *et al.* reported that the upregulation of Sur1- K_{ir}6.2 channels specifically in microglia both in LPS and IFN γ treated cells and also in rat stroke models [23]. On the other hand, Kurland *et al.* demonstrated no change in the expression of the K_{ir}6.2 subunit in microglia stimulated with LPS both *in vitro* and *in vivo* studies [24].

1.2.2. Sur1-Trpm4 Channels

Sur1 can also couple with transient receptor potential cation channel subfamily M member/melastatin 4 (Trpm4) to form the ATP and Ca²⁺ sensitive non selective cation channels [25]. These channels are responsible for Na⁺ influx, therefore opening of the Sur1-Trpm4 channels depolarizes the cell and have been linked to formation of cytotoxic edema [26]. The Sur1-Trpm4 channels are not constitutively expressed in healthy cells, however, they are shown to be prominently upregulated in neurons, astrocytes and cerebral microvascular endothelial cells both in human and *in vivo* stroke models [26-27]. Additionally, Sur1-Trpm4 channels are shown to be upregulated in microvessels and

neurons in both rat model of subarachnoid hemorrhage (SAH) and in brain tissues taken from patients with SAH [28]. Expression of these channel proteins were also elevated in the protein lysates of rodent models of spinal cord injury (SCI) [29]. The upregulation of Sur1-Trpm4 channels in astrocytes has also been reported in the experimental autoimmune encephalomyelitis model [30]. Furthermore, Sur1 is upregulated in neurons, astrocytes, activated microglia/macrophages, neutrophils and capillary endothelial cells in tissues obtained from the pericontusional area in human TBI patients [31]. Similarly, in a rat TBI model, Sur1 was upregulated in neurons and microvascular structures [32]. The specific upregulation of Sur1-Trpm4, but not Sur1- $K_{ir}6.2$ channels has been documented in rat intracerebral hemorrhage (ICH) models [33-34]. Moreover, in a rat encephalopathy of prematurity model, Sur1 upregulation has been shown in periventricular areas, prominently in the microvessels within the subventricular zone [35].

The involvement of the Sur1-Trpm4 channel has been monitored in several disorders of the nervous system and that's why it is important to understand how it causes ionic and vasogenic edema, leading to hemorrhagic transformation (Figure 1.2). Upon an insult to the central nervous system (CNS), the glucose and O_2 supply to the cells may be compromised due to several complications. As a consequence, intracellular ATP is depleted in these metabolically active cells, leading to the failure of the ATP-dependent active (including Na^+/K^+ and Ca^{2+} ATPases) and passive transport systems that are critical in maintaining the vital electrochemical gradient across membranes [36]. The main cause of cell swelling (edema) is initiated with Na^+ influx into the cell, which can be carried out via the NKCC1 cotransporter and the Na^+/H^+ exchanger that works together with the Cl^-/HCO_3^- exchanger [36]. In addition to these, ATP sensitive Sur1-Trpm4 channels are upregulated upon an insult to further promote Na^+ influx into the cell [26]. All these membrane proteins work in coherence to direct Na^+ influx, which in turn brings Cl^- and water into the cell through diffusion. Aquaporin channels maintain the osmotic pressure within the cell. Intracellular accumulation of these solutes have been described in detail as cytotoxic edema, which causes cell blebbing and eventually oncotic cell death [36]. If reperfusion does not occur, cytotoxic edema can deteriorate and cause ionic edema, which is characterized by the transport of Na^+ , Cl^- and water across the BBB [37]. Since the concentration of these solutes are now depleted in the extracellular space, a new concentration gradient is formed for Na^+ , Cl^- and water across the BBB [10]. Accordingly, transendothelial movement of these solutes into the extracellular space cause brain swelling and result in an increase in BBB permeability [36].

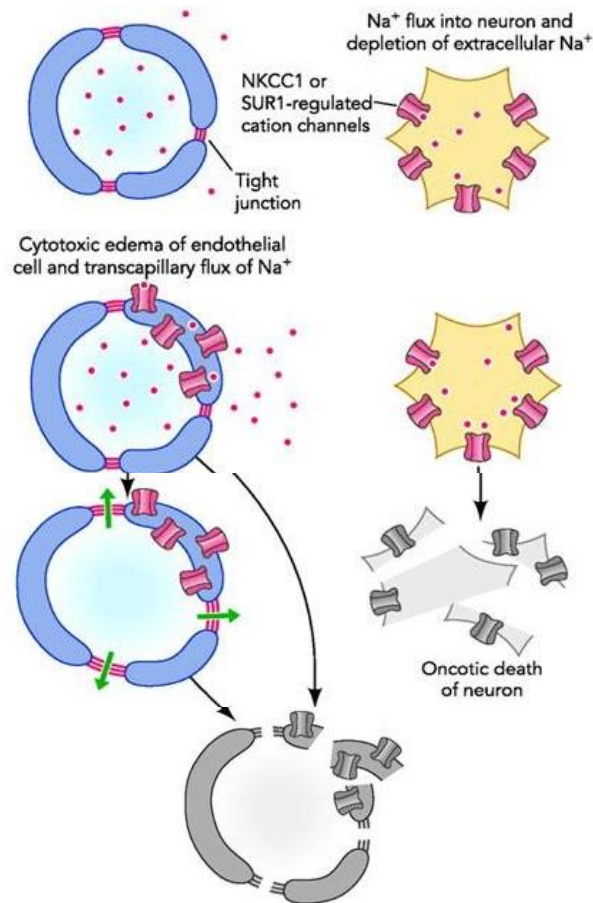


Figure 1.2. Representations of cytotoxic, ionic and vasogenic edema leading to hemorrhagic transformation. After an ischemic injury, Na^+ influx into the neurons through NKCC1 or Sur1-Trpm4 channels cause cytotoxic edema. When Na^+ is depleted in the extracellular space, a new concentration gradient is formed between the intravascular compartment and the capillary wall, which is called ionic edema. Vasogenic edema is caused by the breakdown of the tight junction proteins. Oncotic death of endothelial cells results in BBB leakage and eventually leads to hemorrhagic transformation. (Kahle *et al.* [36])

Increased permeability of endothelial cells causes the extravasation of blood serum proteins, which can be named as vasogenic edema. In this phase, endothelial cells are retracted due to actin polymerization and disruptions are prominently observed in tight junctions and basement membrane proteins [37]. Hemorrhagic transformation, which is lethal in most stroke cases, is observed when the structural integrity of capillaries are completely lost and blood extravasates directly into the brain parenchyma [10].

After an ischemic event, in coherence with the changes in the ionic homeostasis mentioned above, several transcriptional mechanisms are also activated during edema formation, which includes hypoxia inducible factor 1 (HIF1), activator protein 1 (AP1), Sp1 and nuclear factor kappa b (NF- κ B) [37]. Additionally, analysis of the promoter

regions of both *Abcc8* gene, which encodes Sur1, and *Trpm4* gene have revealed that there are several putative consensus sequences for the binding of these transcription factors Sp1, AP1 and NF- κ B [26, 37-38]. Therefore, activation of these transcription factors has been linked to the upregulation of Sur1-Trpm4 channels following an ischemic event, leading to oncotic cell death [39].

1.3. Glibenclamide

Glibenclamide (US name: glyburide) is one of the sulfonyl urea group of drugs, which is an ATP sensitive potassium channel blocker. It has been used to treat diabetes mellitus type 2 (DM 2) for over forty-five years without any adverse side effects in patients [21]. Glibenclamide is capable of inhibiting both Sur1-Trpm4 and Sur1-K_{ir}6.2 channels, and its protective effect was demonstrated in a meta-analysis study when diabetic patients with and without taking glibenclamide were compared after stroke in the USA, Canada and Germany [40]. Since Sur1 has been shown to be upregulated following stroke and CNS injuries, glibenclamide became an ideal candidate for the treatment of these pathological conditions for several reasons: (1) it can pass through the BBB due to leakage in cases of hemorrhagic strokes, (2) it is slightly acidic and lipid soluble, which enhances its penetrance to the brain parenchyma under hypoxic/ischemic conditions [18].

The protective effects of glibenclamide has been demonstrated in *in vivo* models of ischemic stroke, subarachnoid hemorrhage, intracerebral hemorrhage, encephalopathy of prematurity, traumatic brain injury and spinal cord injury [32-33, 35, 41-44]. It has been shown that glibenclamide reduces infarct volume and edema, prevents neuronal death and associated secondary hemorrhages, and attenuates neurobehavioral outcomes. Human clinical trials of glibenclamide is ongoing for ischemic stroke patients on phase III level and for TBI patients on phase II level (<https://clinicaltrials.gov>; NCT numbers for stroke: NCT01794182 and NCT02864953; NCT number for TBI: NCT01454154).

In addition to stroke and CNS injuries, the protective effect of glibenclamide has been shown in lipopolysaccharide (LPS) stimulated rats, where glibenclamide reversed the LPS induced hypotension and inhibited the expression of inducible nitric oxide synthase, which ameliorates the outcome [45-46].

1.4. TLR4 Signaling

Pattern recognition receptors (PRRs) take role in the innate immune system and recognize foreign cells or molecules namely, pathogen associated molecular patterns (PAMPs) and danger associated molecular patterns (DAMPs). Peculiar to the PRRs, repeating leucine rich motifs are found at their extracellular domain^[47]. Toll like receptor (TLR) is also part of the PRR family and possess an evolutionarily conserved toll/interleukin 1 receptor (TIR) domain, which includes three homology regions named as boxes^[48-49]. In addition to its TIR domain, TLRs have leucine rich region motifs on their extracellular side^[49]. Thus far, there are eleven different TLRs in human and twelve in mouse that have been identified^[50]. Among them, TLR2 and TLR4 can specifically recognize PAMPs such as LPS and TLR4 still remains to be the most widely studied receptor^[49]. LPS is found on the outer membrane of Gram-negative bacteria and it incorporates two portions: Lipid A and an oligosaccharide. Lipid A is the fundamental part of LPS, which causes cells to give an inflammatory response^[51].

After TLR4 activation, cells can use the Myd88 dependent and/or the Myd88 independent signaling pathways. In both ways, TLR4 can induce proinflammatory and apoptotic signals by secreting tumor necrosis factor alpha (TNF α), interleukin (IL) 1 β and IL6 and increase the production of reactive oxygen species (ROS) and nitric oxide (NOS)^[51-52]. LPS induced TLR4 signaling is also associated with an increased intercellular calcium concentration, which triggers TNF α release in primary Kupffer cells^[53]. Additionally, TLR4 can also induce the upregulation of anti-inflammatory IFN β via the Myd88 independent pathway. Even though it is not known how TLR4 signaling prefers cell survival or cell death in its downstream pathways, proinflammatory cytokines mostly exaggerate the situation leading to cell death^[54].

Because TLR4 expression mainly takes place in microglial cells, LPS has been widely used in microglia for TLR4 signaling studies and its molecular mechanism has been well-established both *in vitro* and *in vivo*^[56-57]. In addition to microglial cells, endothelial cells have also been used in LPS studies to reveal their response to an inflammatory stimuli^[52]. Even though different endothelial cell lines such as human coronary artery, lung microvascular and umbilical cord vein endothelial cells have been investigated upon LPS stimulation, studies with brain microvascular endothelial cells are limited and needs to be further studied^[58-60].

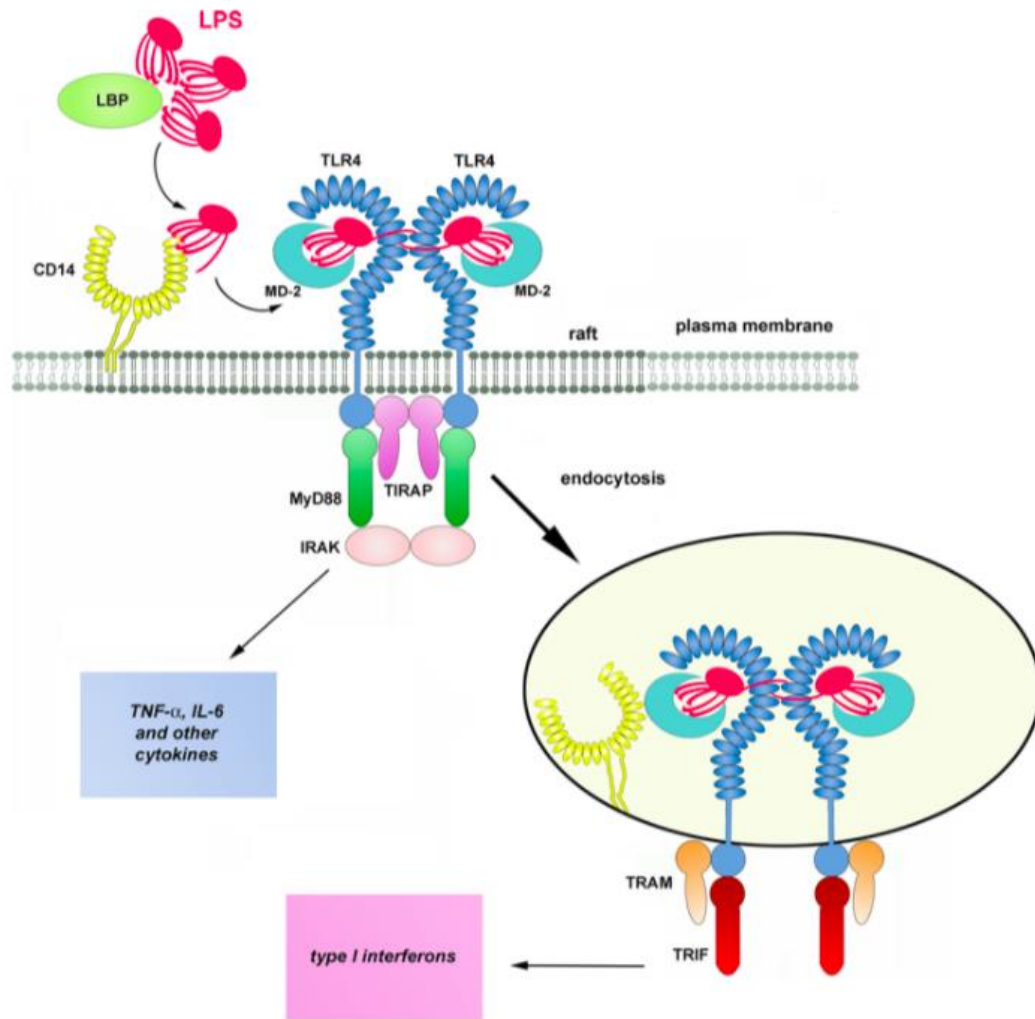


Figure 1.3. LPS activates TLR4 signaling in Myd88 dependent and independent pathways. With the help of CD14 and LBP, LPS is transferred to the TLR4/MD2 complex. Activated TLR4 can recruit the Myd88 protein, which in turn can interact with IRAK and TIRAP molecules, leading to the expression of TNF α and other cytokines. On the other hand, activated TLR4 can undergo endocytosis and interact with TRAM and TRIF molecules, which leads to the expression of type I interferons. (Płociennikowska *et al.* [55])

1.4.1. TLR4 Activation

LPS is recognized by the TLR4 receptor in the host cell with the help of LPS binding protein (LBP). LBP binds LPS and brings it towards TLR4 on the cell membrane. Additionally, LBP interacts with cluster of differentiation 14 (CD14), and forms LPS-LBP-CD14 complex. CD14 has two forms: the first one is mCD14, a GPI anchored membrane protein and the second one is sCD14, a soluble protein without the GPI anchor [51]. CD14 is expressed by some cells like monocytes and macrophages and the presence

of the sCD14 promotes ligand-receptor recognition and the transfer of LPS to myeloid differentiation factor (MD) 2, which is associated with TLR4 through disulfide forming Cys95 residue^[55, 61]. MD2 also helps with the recognition of LPS by TLR4 and transduces the signal, which eventually leads to activation of phosphoinositide 3-kinase (PI3K) and mitogen activated protein kinase (MAPK), and to translocation of NF- κ B. Upon LPS binding, TLR4 dimerizes and recruit adaptor proteins via its cytoplasmic TIR domains^[55]. After TLR4 activation, LPS signal can be transduced via the Myd88-dependent and Myd88-independent pathways.

1.4.2. Myd88 Dependent Signaling

Once the TLR4 receptor is activated, it can attract the Myd88 adaptor protein. Myd88 has a dual role in interacting with the TLR4 receptor through TIR domain and at the same time can simultaneously attract the IL1 receptor associated kinases (IRAK) 1 and 4 through its death domains (DD)^[47]. After the phosphorylation of IRAK1 by IRAK4 and autophosphorylation of IRAK1, IRAK1 becomes activated and can bind the TNF α receptor associate factor (TRAF) 6^[48]. TRAF6 is able to phosphorylate IKK, which in turn can phosphorylate I κ B, the inhibitor of NF- κ B in the cytoplasm, leading to the degradation of I κ B through ubiquitination^[52]. After that, NF- κ B is released from I κ B, and can translocate into the nucleus to induce proinflammatory cytokines, such as TNF α , IL1 β and IL6^[51]. Simultaneously, Myd88 can also attract the TIR domain containing adaptor protein (TIRAP), TIRAP can further interact with both IRAK2 and TRAF6. Once TRAF6 is activated, it can induce an early stage NF- κ B nuclear translocation either via the I κ B or PI3K signaling pathways. Alternatively, it can activate MAPK, leading to AP1 gene expression^[48]. The fate of a cell is ultimately determined by the critical balance between proinflammatory/apoptotic and cell survival signals which are induced by NF- κ B/MAPK and PI3K, respectively^[48].

1.4.3. Myd88 Independent Pathway

The Myd88 independent pathway has been characterized in studies of LPS exposure in Myd88 KO mice, in which the late activation of NF- κ B and MAPK pathways

has been reported ^[62]. In the Myd88 independent way, TLR4 attracts the adaptor molecule TRAM through its TIR domain, which in turn activates TRIF. TRIF is then able to associate with both TRAF3 and TRAF6, where TRAF3 uses IRF3 to induce anti-inflammatory IFN β , and TRAF6 activates late NF- κ B and MAPK pathways ^[54].

1.5. Aim and Hypothesis

In this study, our aim was to show the protective effect of glibenclamide in LPS stimulated bEnd.3 cells. We hypothesize that LPS causes inflammation and cell death via opening of Sur1-Trpm4 channels and glibenclamide reduces the inflammation and cell death caused by LPS.

CHAPTER 2

MATERIALS AND METHODS

2.1 Materials

All materials that are used in the experiments were specified in the methods section.

2.2 Methods

All methods that are used in the experiments were specified in detail in the following sections.

2.2.1 Cell Culture

bEnd.3 cells (ATCC, CRL-2299) were cultured in DMEM medium (Biological Industries, 01-055-1A) supplemented with 10% fetal bovine serum (FBS) (Biological Industries, 04-127-1B), 4 mM L-glutamine (Biological Industries, 03-020-1B) and 100 U/ml penicillin/streptomycin at 37 °C in a humidified atmosphere containing 5% CO₂ (Thermo Scientific, Steri-Cycle Incubator). The medium of cells was changed every 3-4 days and cells were mainly grown in 100 mm petri dishes (Corning, 430167).

2.2.2 Subculturing

After cells reached 80% confluency, they were subcultured for further experiments. Firstly, cell medium was removed, and cells were washed with complete medium and Dulbecco's phosphate buffered saline (DPBS) (Biological Industries, 02-023-1A). After that, cells were trypsinized with 0.25% Trypsin – 0.02% ethylenediaminetetraacetic acid (EDTA) solution (Biological Industries, 03-050-1B) and incubated for 5 minutes at 37 °C. After pipetting the detached cells, they were neutralized

with equal volume of complete medium and collected in 15 ml falcon tubes (Jet-Biofil, CFT-011-150). Cells were centrifuged (Nüve, NF800R) at 700 rpm for 5 minutes, and then excess medium was removed. Cells were dissolved in 1 ml complete medium and 16 μ l of cells were mixed with 64 μ l 0.4% Trypan blue (Sigma, T6146) in DPBS. 40 μ l of the cell and dye mixture was loaded into each side of the hemocytometer (Isolab, 075.03.002) and cells were counted by using Olympus inverted microscope (IX81) at 10X magnification. The total cell number was determined by using the following calculation:

$$\text{Cells/ml} = \text{Average of cell counts} \times 5 \times 10^4$$

The desired number of cells were diluted with complete medium and seeded accordingly depending on the specific experiment (Table 2.1).

Table 2.1. The seeding numbers of cells in different types of culture plates.

Culture Plate	Seeding Number
96 Well plate	5,000
48 Well plate	25,000
24 Well plate	50,000
12 Well plate	100,000
6 Well plate	300,000
100 mm dish	800,000

2.2.3 Cell Freezing and Thawing

10% dimethyl sulfoxide (DMSO) (AppliChem, A3672) in FBS was prepared as freezing medium and approximately 7×10^5 trypsinized cells were transferred slowly into cryovials containing the freezing medium. The vial was stored in $-20\text{ }^{\circ}\text{C}$ for several hours and then it was transferred to the $-80\text{ }^{\circ}\text{C}$ freezer (Nüve, DF490).

When required, frozen vials of cells from $-80\text{ }^{\circ}\text{C}$ were incubated in a $37\text{ }^{\circ}\text{C}$ water bath (WiseBath, WB-22) until the cells were completely defrosted. Cells were then plated into 100 mm petri dishes containing complete medium. The medium of cells was changed

with fresh media the following day, and cells were maintained as described previously at 2.2.1.

2.2.4 Propidium Iodide and Hoechst Staining

5,000 cells per well were seeded into 96 well culture plates (Costar, 3599) in triplicates, with the total volume being 200 μ l/well. The following day, old medium was removed, and cells were washed with serum free medium (SFM). After that, cells were assigned to five groups; as (i) control, (ii) LPS, (iii) LPS+Glibenclamide, (iv) Glibenclamide and (v) DMSO. For all propidium iodide labeling experiments the concentrations of LPS and glibenclamide were kept constant: 1 μ g/ml LPS (Invivogen, tlr1-3pelps) and 30 μ M glibenclamide (Sigma, G2539) in DMSO was dissolved in serum free medium and added to each well, as appropriate. Only serum free media was added to the control group and only same volume of DMSO as glibenclamide was added to cells in the DMSO group to test the solvents effects on cells. All cells were incubated with their respective reagents for 6, 12, 24 and 48 hours following LPS treatment. After the completion of the incubation period, dead cells were stained with propidium iodide (Sigma, P4170; ratio: 1/500) and all cells were stained with Hoechst (Sigma, B2261; ratio: 1/50) solution that was added to each well and cells were incubated for 30 minutes at 37 °C in dark. After staining, cell images were taken with the Olympus inverted microscope (IX83) at 4X magnification. Dead and alive cells were counted with the ImageJ Software (NIH, 1.52n).

In all experiments, where LPS was involved, serum free medium was used for all groups. The main reason behind this was to increase the efficacy of glibenclamide, which has been shown to be 99% protein bound ^[63]. Additionally, several growth factors and hormones within FBS may promote cell proliferation, manipulating the total cell number of control and treated groups ^[64].

2.2.5 Protein Isolation

800,000 cells were seeded in triplicates in 100 mm petri dishes containing complete medium and cells were incubated at 37 °C overnight. The following day, old medium was removed, and cells were washed with serum free medium. Next, plates were

assigned to three groups, as (i) control, (ii) LPS and (iii) LPS+Glibenclamide. For protein isolation studies, the concentrations of LPS and glibenclamide were kept constant: 1 µg/ml LPS and 30 µM glibenclamide were dissolved in 8 ml serum free medium, as appropriate. All plates were incubated at 37 °C for 6, 12, 24 and 48 hours following LPS treatment.

After the appropriate incubation period was completed, plates were placed on ice and cells were scraped with a sterile cell scraper. The cells along with the media were transferred into 15 ml falcon tubes, and they were collected by centrifugation at 4,100 rpm for 5 minutes at room temperature (RT). The supernatant was collected for further experiments and the pellet was transferred into 1.5 ml Eppendorf tube after dissolving in 200 µl medium. Next, cells were collected in a pre-cooled 4 °C centrifuge (VWR, Micro Star 17R) at 5,000 rpm for 5 minutes. The pellet was washed with 200 µl ice-cold phosphate buffered saline (PBS) (Sigma, P4417) and centrifuged again at 5,000 rpm for 5 minutes at 4 °C. Then, the pellet was dissolved in 20 µl lysis buffer solution, containing 1X radioimmunoprecipitation assay buffer (RIPA buffer) (Table 2.1) with protease inhibitor cocktail (Roche, 04693159001). Cells were incubated on ice for 30 minutes and vortexed every 5 minutes during this period. Next, cells were centrifuged at 14,000 g for 15 minutes at 4 °C and the supernatant was transferred into fresh tubes.

Table 2.2. 2X RIPA buffer recipe

Reagents	Brand Name and Catalog Number
0.1 % Sodium dodecyl sulfate (SDS)	Fisher BioReagents BP166
% Triton X-100	AppliChem, 9002-93-1
2 mM EDTA	Sigma, E5134
140 mM NaCl	Emsure, 1.06404
10 mM Tris (pH:8)	AppliChem, 77-86-1

2.2.6 Determination of Protein Concentration by BCA

1, 0.8, 0.6, 0.4, 0.2 and 0.1 mg/ml bovine serum albumin (BSA) (BioShop, ALB001.50) standards were prepared water and protein samples were 1:25 diluted, both in ultra-pure water. 25 µl from BSA and protein samples were loaded into 96 well culture plate in duplicates. 25 µl ultra-pure water was used as blank. 200 µl of BCA solution

mixture (Pierce, 23227) containing reagent A and reagent B (ratio: 50:1), was prepared and was added to all samples and standards. Then, 96 well culture plate was incubated at 37 °C for 30 minutes. Finally, the absorbance values were measured at 562 nm by using Thermo Scientific Multiskan Spectrum and absorbance value of blank was subtracted from all samples prior to any calculations. A standard curve was constructed by using the BSA standards, and the unknown protein concentrations were determined by fitting the absorbance value to the equation generated for each individual experiment.

2.2.7 Western Blotting

4X loading dye was prepared by mixing 40 mM Tris (pH:8), 0.4 mM EDTA and 4% SDS. Protein samples were mixed with the loading dye and incubated at 95 °C for 5 minutes to denature samples. 1 mm 8%-12% sodium dodecyl sulphate polyacrylamide gel electrophoresis (SDS-PAGE) gels were prepared by polymerizing the separating and stacking gels (Table 2.3 and Table 2.4) with 4X resolving and stacking buffers (Table 2.5 and Table 2.6) and placed into running tank (BioRad Mini-PROTEAN Tetra Cell, 1658001) containing 1X running buffer (Table 2.7). Then, equal amounts of protein samples along with 5 µl protein marker (Thermo Scientific, 26619) were loaded and separated in the 8%-12% SDS-PAGE gels at 90 Volts (constant voltage) for 90 minutes by using Biorad, PowerPac Basic Power Supply. Next, gels were transferred to PVDF membranes (Roche, 03010040001) in 1X transfer buffer (Table 2.8) at 100 Volts (constant voltage) for 2-3 hours, depending on the protein size. After the transfer was completed, membranes were blocked in 5% milk in 1X tris buffered saline 0.1% Tween-20 (TBS-T) (Table 2.9) for 1 hour at RT on an orbital shaker (Thermo Scientific, 88881101). Then, membranes were incubated with primary antibodies (Table 2.10), which was dissolved in 5% milk in TBS-T overnight on an orbital shaker (Thermo Scientific, 88880026) at 4 °C. The following day, after several rinses in TBS-T, membranes were incubated with anti-mouse immunoglobulin horseradish peroxidase (HRP) conjugated secondary antibody (Amersham, NA931; ratio: 1/5,000) in 5% milk in TBS-T for 1 hour at RT. After several rinses in TBS-T, membranes were developed with enhanced chemiluminescence (ECL) substrate working solution (Thermo Scientific, SuperSignal West Pico). Finally, the observed bands were quantified by using Image Studio Lite Software and all samples were normalized to γ -tubulin as a loading control.

2.2.8 Immunostaining

50,000 cells were seeded in 24 well culture plates (SPL) containing 500 μ l complete medium and cells were incubated at 37 °C overnight. The following day, old medium was removed, and cells were washed with serum free media. Next, wells were assigned into three groups, as (i) control, (ii) LPS and (iii) LPS+Glibenclamide groups. 500 μ l of serum free medium was added to the control group and 1 μ g/ml LPS in 500 μ l serum free medium was added to the LPS group. 1 μ g/ml LPS and 30 μ M glibenclamide in 500 μ l serum free medium was added to LPS+Glib group and all plates were incubated at 37 °C for 24 and 48 hours following LPS treatment.

Control, LPS and LPS+Glib cells were fixed with 4% paraformaldehyde (PFA) (Sigma, P6148) in 1X PBS at room temperature for 15 minutes and then washed with 1X PBS for several times. Next, cells were blocked with 2% normal donkey serum (Sigma, D9663), in 0.2% Triton X-100 (Applichem, 9002-93-1) in 1X PBS for 1 hour at room temperature. Cells were incubated with cleaved Caspase-3, NF κ B, ZO-1 and COL IV primary antibodies (Table 2.10) overnight at 4°C on a shaker. The following day, cells were washed several times with 1X PBS for an hour, and cells were then incubated with species appropriate secondary antibodies (Table 2.11) in blocking solution in dark for 1 hour at room temperature. After washing cells with 1X PBS for 2 hours, 0.1% DAPI solution (Sigma) was added as a counterstain and incubated for 15 minutes at room temperature. Omission of primary antibody was used as a negative control and images of cells were captured with Olympus inverted microscope and processed with ImageJ software. All pictures for every antibody were taken at the same magnification, exposure and gain settings for unbiased image analysis, including negative controls.

Table 2.3. Separating gel recipe for different percentages (For 10 ml)

Reagents	8%	10%	12%
30% Acrylamide	2.7 ml	3.3 ml	4.0 ml
4X Resolving buffer	2.5 ml	2.5 ml	2.5 ml
10X APS (Sigma, 215589)	100 μ l	100 μ l	100 μ l
TEMED (AppliChem, A1148)	6 μ l	4 μ l	4 μ l
dH ₂ O	4.7 ml	4.1 ml	3.4 ml

Table 2.4. Stacking gel recipe

Reagents	Volumes
30% Acrylamide	425 μ l
4X Stacking buffer	625 μ l
10X APS (Sigma, 215589)	25 μ l
TEMED (AppliChem, A1148)	5 μ l
dH ₂ O	1.425 ml

Table 2.5. 4X Resolving buffer (For 200 ml)

Reagents	Brand Name and Catalog Number
1.5M Tris base	AppliChem, 77-86-1
0.4% SDS	Fisher BioReagents BP166
pH	8.8
dH ₂ O	Add up to 200 ml

Table 2.6. 4X Stacking buffer (For 200 ml)

Reagents	Brand Name and Catalog Number
0.5M Tris base	AppliChem, 77-86-1
0.4% SDS	Fisher BioReagents BP166
pH	6.8
dH ₂ O	Add up to 200 ml

Table 2.7. 10X Running buffer recipe (For 500 ml)

Reagents	Brand Name and Catalog Number
15 g Tris base	AppliChem, 77-86-1
72 g Glycine	Fisher Bioscientific, BP381
5 g SDS	Fisher BioReagents BP166
dH ₂ O	Add up to 500 ml

Table 2.8. 1X Transfer buffer recipe (For 500 ml)

Reagents	Brand Name and Catalog Number
1.5 g Tris base	AppliChem, 77-86-1
7.2 g Glycine	Fisher Bioscientific, BP381
20% Methanol	İron Kimya
dH ₂ O	Add up to 500 ml

Table 2.9. 1X TBS-0.1% Tween-20 recipe (For 500 ml)

Reagents	Brand Name and Catalog Number
1.2 g Tris base	AppliChem, 77-86-1
4.4 g NaCl	Emsure, 7647-14-5
500 µl Tween 20	AppliChem, 9005-64-5
dH ₂ O	Add up to 500 ml

Table 2.10. Primary antibody list (IF: Immunofluorescence, WB: Western blotting)

Antibody	Ratio	Host	Brand Name	Catalog Number
Cleaved Caspase-3	1:200 for IF	Mouse	Cell Signaling	9661
	1:1,000 for WB			
γ-tubulin	1:10,000	Mouse	Sigma	T6557
NFκB	1:200	Rabbit	Santa Cruz	SC372
ZO-1	1:100	Mouse	Invitrogen	339100
COL IV	1:400	Rabbit	Abcam	6586

Table 2.11. Secondary antibody list

Antibody	Conjugate	Ratio	Brand Name	Catalog Number
Goat anti mouse	Alexa Fluor 488	1:400	Invitrogen	A11029
Donkey anti rabbit	Alexa Fluor 555	1:400	Invitrogen	A31572

2.2.9 Image Analysis with ImageJ

b.End3 cells that have been exposed to 1 µg/ml LPS for various time points and some that have been treated with glibenclamide (30uM) were fluorescently labelled, and

all images were taken with fluorescent microscope to compare these two groups with their time-appropriate controls. For the analyses of collagen IV and zonula occludens 1, total mean intensity was calculated by using the ImageJ Software for each image for all groups. Then, the mean intensities were used for further statistical analyses.

For the analyses of cleaved caspase-3 and NFκB on ImageJ, corresponding DAPI stained images were used as a reference to label each nucleus in the image that was later designated as region of interest (ROI) (Figure 2.1). For this purpose, a threshold value was set, where all nuclei within the image were distinguishable and same threshold value was applied to all DAPI images. When required, Erode, Dilate and Watershed options, under the tab of Process > Binary, were used and after that Particle Analyze was performed on each DAPI image. The corresponding image (labelled with either NFκB or cleaved caspase 3) was opened in ImageJ. Next, the tick of Show All option on the ROI manager was removed and labelled again. By using Measure on ROI manager, mean intensity within each nucleus was calculated for all of the cells in the respective image. Finally, mean intensity of the background was calculated for each image and the threshold was set to 3 times this intensity. The percent ratio was calculated by dividing the number of cells whose intensities are above this value by the total cell number for each image.

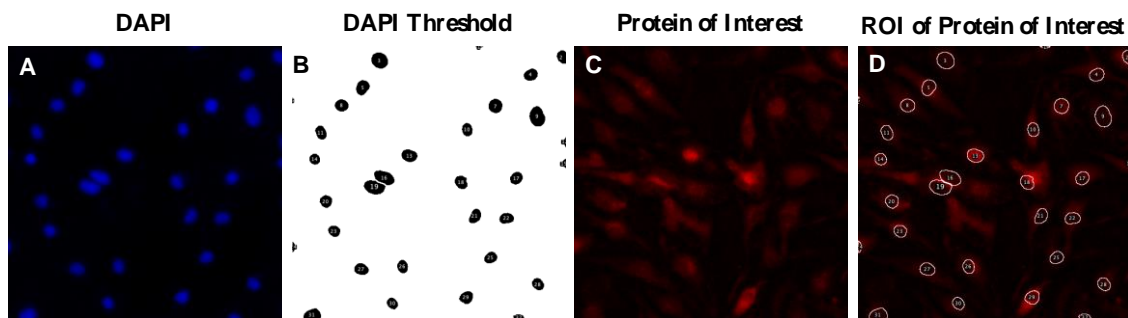


Figure 2.1. Image analysis of NFκB on ImageJ. A) DAPI image, which is going to be used as a reference to label each nucleus in the image. B) Particle analyze is performed to define ROI, after applying Threshold, Erode, Dilate and Watershed on DAPI image. C) NFκB or cleaved caspase-3 image, whose mean intensity for each nucleus is going to be calculated. D) NFκB or cleaved caspase-3 image, which represents ROI of each nucleus.

For the analyses of propidium iodide and Hoechst staining, Hoechst images were blurred by Gaussian Blur option, under the tab of Process > Filter and saved (Figure 2.2). Generally, images were blurred by 10.0, however based on the image different values can be set. Then, Image Subtraction was used in order to subtract the blurred image from the

original Hoechst image. Subtracted image was subjected to Threshold change, until all nuclei became visible in the image, and then the image was further processed with Erode, Dilate and Watershed options, under the tab of Process > Binary. Next, variance filter was used with 1.0, under the tab of Process > Filter, and image was further processed with Fill Holes, Erode, Dilate and Watershed options. Finally, Particle Analyze was performed and the total cell number was recorded. The same process was performed for propidium iodide stained images as well, by using the same threshold value that was used for Hoechst image. % cell death was calculated by dividing the number obtained from propidium iodide image by the number obtained from Hoechst image and multiplied by 100.

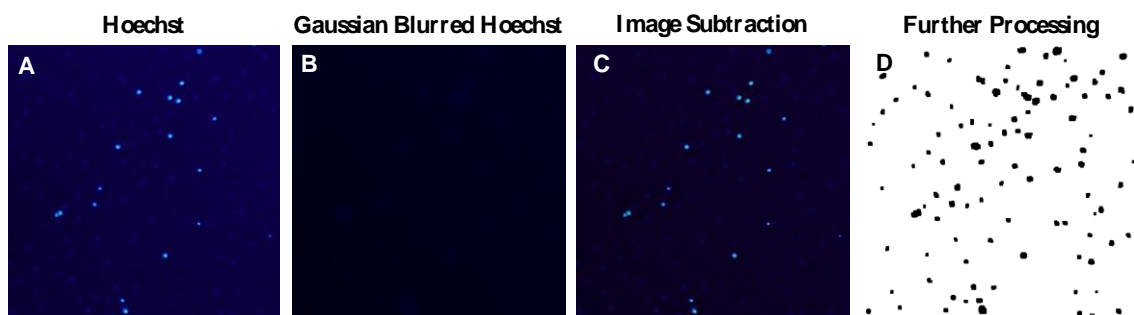


Figure 2.2. Image analysis of Hoechst stained images via ImageJ. A) Hoechst image, whose total cell number is going to be calculated. B) Gaussian blurred version of Hoechst image. C) Gaussian blurred image is subtracted from the original Hoechst image. D) Subtracted image is further processed by applying different settings. (Same analysis is performed for propidium iodide stained images to calculate the total number of dead cells.)

2.2.10 Statistical Analysis

All data was presented as mean \pm standard error of mean (SEM). Student's t-test was used when comparing the immunostaining and Western blot analyses of cleaved caspase-3 between control and LPS groups. Analysis of variance (ANOVA) with post-hoc Tukey test was used when comparing the cell death via propidium iodide and Hoechst staining among control, LPS, LPS+Glib, Glib and DMSO groups. For the rest of the statistical analyses, analysis of variance (ANOVA) with post-hoc Tukey test was used. Any difference among groups was assumed to be significant, when p value is less than 0.05. All statistical analyses were performed by using GraphPad Prism 5.0 (GraphPad Software, Inc., San Diego, CA).

CHAPTER 3

RESULTS

3.1 Investigation of Cell Death via Cleaved Caspase-3 Expression in LPS Stimulated bEnd.3 cells

Inflammation due to LPS stimulation causes apoptosis in liver vascular endothelial, renal tubular cells, lymphocytes, bone marrow derived macrophages, dermal microvascular endothelial, lung endothelial, glomerular endothelial, umbilical vein endothelial cells^[65-71]. That is why we first wanted to see whether LPS stimulated bEnd.3 cells had increased levels of cleaved caspase-3 protein expression via two independent techniques, by Western blotting and immunostaining.

For cleaved caspase-3 immunostaining experiments, bEnd.3 cells were exposed to 1 µg/ml LPS for 24 hours. Our results reveal that the cells stimulated with LPS showed a 4.7-fold increase in the activated caspase-3 protein amount, when compared to control cells (Figure 3.1).

Furthermore, we investigated the expression pattern of cleaved caspase-3 by Western blot after bEnd.3 cells were stimulated with 1 µg/ml LPS in a time dependent manner. 6 hours LPS stimulated bEnd.3 cells had 1.2 times more cleaved caspase-3 expression, which was not statistically different from the control group (Figure 3.1). On the other hand, LPS incubation of bEnd.3 cells for 24 hours showed a 2.5-fold increase in the activated caspase-3 levels when compared to controls (Figure 3.1). Additionally, glibenclamide was able to significantly reduce the amount of cleaved caspase-3 to control levels after 24 hours of LPS stimulation (Figure 3.1). LPS incubation of bEnd.3 cells for 48 hours showed a 5.0-fold increase in the activated caspase-3 levels when compared to the control group (Figure 3.1). Moreover, glibenclamide was able to significantly reduce the amount of cleaved caspase-3 at 48 hours, yet it was still observed to be 2.6 times more than the control group (Figure 3.1).

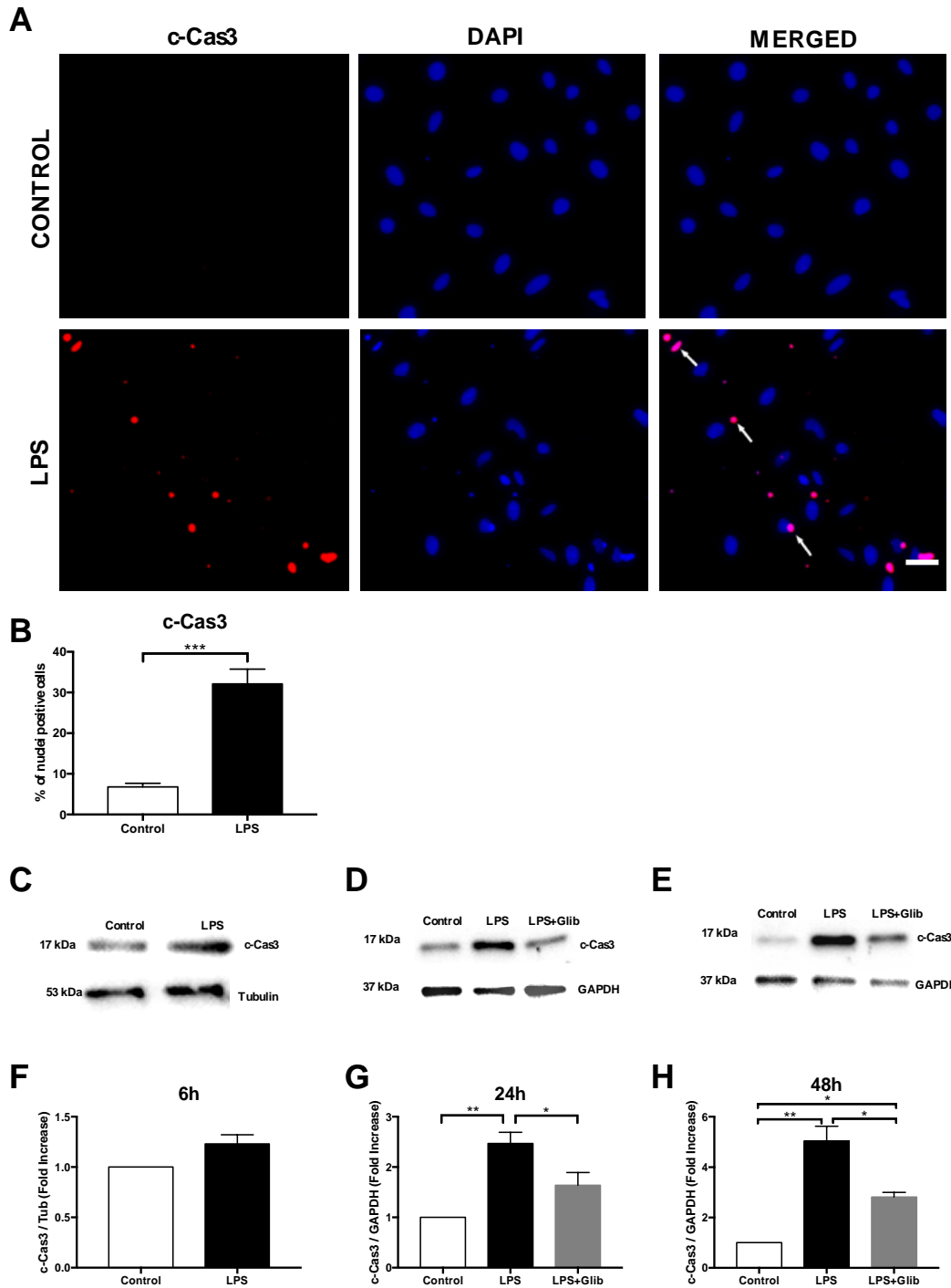


Figure 3.1. Cleaved caspase-3 is upregulated in bEnd.3 cells after LPS stimulation. A) Representative images and B) quantitative analysis of cleaved caspase-3 of control and 1 $\mu\text{g/ml}$ LPS stimulated cells after 24 hours. C) Expressions and F) quantitative analysis of cleaved caspase-3 from 6 hours control and 1 $\mu\text{g/ml}$ LPS stimulated bEnd.3 cells. Expressions and quantitative analysis of cleaved caspase-3 from 24 (D-G) and 48 (E-H) hours control, 1 $\mu\text{g/ml}$ LPS and 1 $\mu\text{g/ml}$ LPS + 30 μM Glibenclamide incubated bEnd.3 cells. Tubulin/GAPDH is used as a loading control for Western blot. Results are given as mean \pm SEM; n=3 for Western blot experiments. (* $p < 0.05$; ** $p < 0.01$; *** $p < 0.001$) Arrows show cleaved caspase-3 positive cells. Scale Bar: 50 μm .

3.2 Determination of Cell Death via Propidium Iodide and Hoechst Staining

The effect of glibenclamide on cell death was determined via propidium iodide and Hoechst staining in bEnd.3 cells after LPS stimulation. LPS stimulated cells were exposed to 1 $\mu\text{g/ml}$ LPS, and the glibenclamide treated group (LPS+Glib) was incubated in 30 μM glibenclamide as LPS (1 $\mu\text{g/ml}$) was introduced to the media. Some cells were solely treated with 30 μM glibenclamide to observe the effect of drug treatment alone. The effect of DMSO on bEnd.3 cells was also evaluated, as glibenclamide was dissolved in DMSO as a solvent. All images were taken by fluorescent microscope and percent cell death was calculated for all groups, at 6, 12, 24 and 48 hours following LPS stimulation.

There was no significant difference in the calculated percent cell death among groups at 6 and 12 hours after LPS exposure (Figure 3.2A and 3.2B). The percent cell death significantly increased from 10.9 % to 15.9 % 24 hours after LPS stimulation, and glibenclamide was able to reduce this down to 8.5 % at the same time-point (Figure 3.2C). 48 hours following LPS exposure, percent cell death in LPS treated cells increased significantly from 11.4 % to 16.0 % when compared to controls, and glibenclamide reduced cell death to 11.2 % (Figure 3.2D). These findings reveal that glibenclamide is able to restore cell death induced by LPS 24 and 48 hour after stimulation in bEnd.3 cells. Furthermore, no significant differences were observed between control, glibenclamide alone and DMSO groups at both 24 and 48 hours, indicating that DMSO alone did not cause cell death in bEnd.3 cells, and glibenclamide alone was not protective in bEnd.3 cells by itself.

3.3 The Effect of Glibenclamide on NF κ B Translocation

The effect of glibenclamide on NF κ B nuclear translocation was demonstrated with immunostaining in bEnd.3 cells 24 and 48 hours after LPS stimulation. The exposure of cells to LPS for 24 hours caused NF κ B to translocate to the nucleus \cong 5.3 times more, when compared to controls at the same time-point (Figure 3.3). On the other hand, glibenclamide was able to significantly suppress this nuclear localization by 45%, when compared to the LPS treated cells (Figure 3.3). It is also interesting to note that nuclear

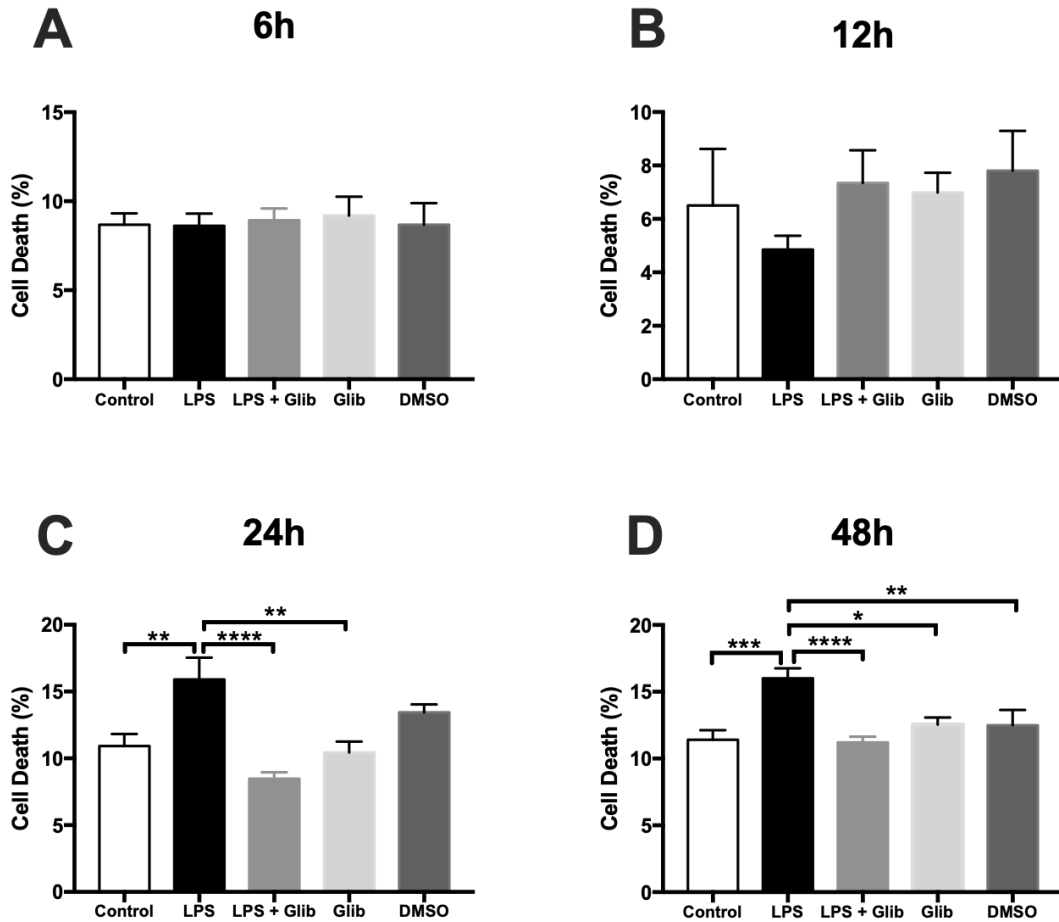


Figure 3.2. The effect of glibenclamide on cell death in LPS stimulated bEnd.3 cells. Propidium iodide and Hoechst staining in A) 6 hours incubation, B) 12 hours incubation, C) 24 hours incubation and D) 48 hours incubation with 1 $\mu\text{g/ml}$ LPS and/or 30 μM glibenclamide. For DMSO groups, DMSO is included in the media of cells with the same volume as glibenclamide. All experiments are performed in triplicates and results are given as mean \pm SEM; $n=3$. (* $p<0.05$; ** $p<0.01$; *** $p<0.001$; **** $p<0.0001$)

translocation of NF κ B was not significantly different between the control and LPS+Glib groups. ($p = 0.0969$)

Similarly, the exposure of cell to LPS for 48 hours caused NF κ B to translocate into the nucleus $\cong 5.3$ times more, when compared to control cells (Figure 3.4). On the other hand, glibenclamide was able to significantly suppress this nuclear localization by 26 % when compared to LPS treated cells (Figure 3.4). Additionally, glibenclamide treatment was not sufficient to completely block this translocation as a significant increase was still detected when compared to controls.

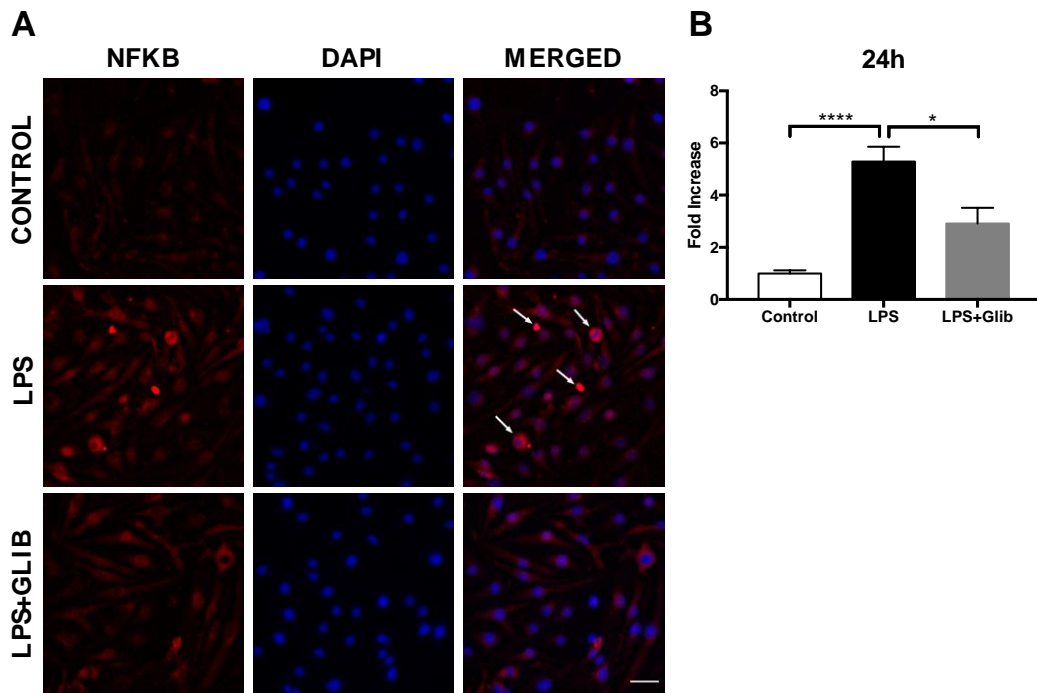


Figure 3.3. Glibenclamide reduces the amount of NFκB translocation into the nucleus in 24 hours LPS stimulated bEnd.3 cells. A) Representative NFκB, DAPI and merged images are from control, LPS and LPS+Glib groups. B) Quantitative NFκB analysis of images is demonstrated for 24 hours LPS incubation. Results are given as mean ± SEM; n=3. (*p<0.05; ****p<0.0001) Arrows show NFκB translocation. Scale Bar: 50 μm.

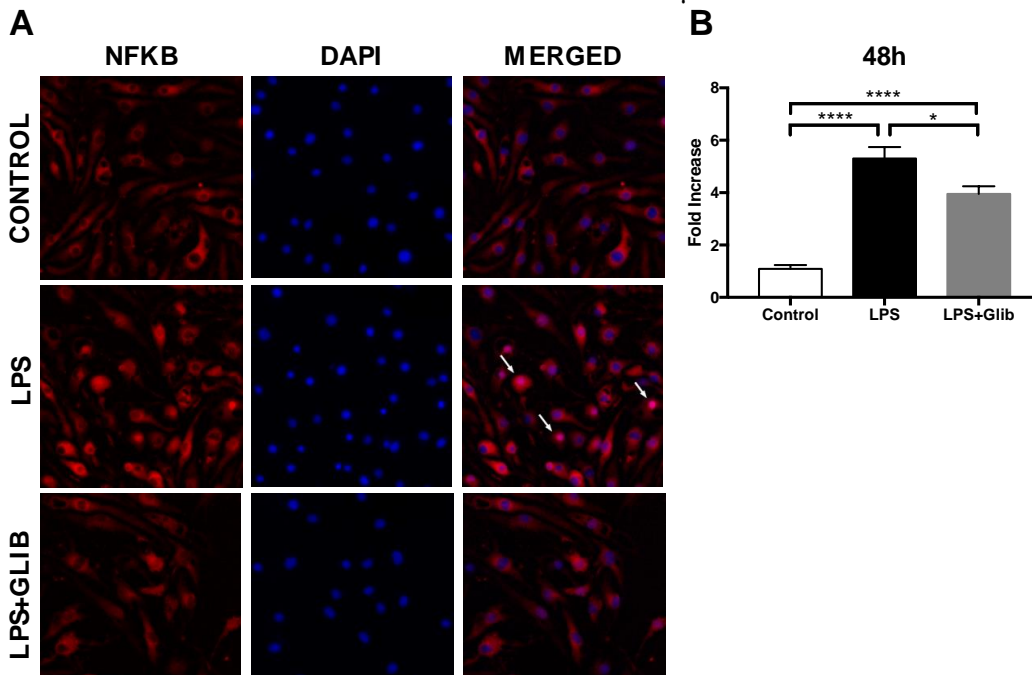


Figure 3.4. Glibenclamide reduces the amount of NFκB translocation into the nucleus in 48 hours LPS stimulated bEnd.3 cells. A) Representative NFκB, DAPI and merged images are from control, LPS and LPS+Glib groups. B) Quantitative NFκB analysis of images is demonstrated for 48 hours LPS incubation. Results are given as mean ± SEM. (*p<0.05; ****p<0.0001) Arrows show NFκB translocation. Scale Bar: 50 μm.

3.4 The Effect of Glibenclamide on Collagen IV in LPS Stimulated bEnd.3 Cells

The effect of glibenclamide on collagen IV, which is one of the basal lamina proteins, was investigated by immunostaining at 24 and 48 hours after bEnd.3 cells were stimulated with LPS.

There was no significant difference in the collagen IV amount among control, LPS and LPS+Glib treated groups 24 hour after LPS exposure (Figure 3.5). On the other hand, collagen IV expression levels in cells that were exposed to LPS for 48 hours dropped significantly by $\cong 40\%$ when compared to controls. Furthermore, glibenclamide was able to recover the expression of collagen IV in these cells by $\cong 77\%$, when compared to the LPS group (Figure 3.6). Additionally, control and LPS+Glib groups were not significantly different from each other. ($p = 0.4614$)

3.5 The Effect of Glibenclamide on Zonula Occludens-1 in LPS Stimulated bEnd.3 cells

The effect of glibenclamide on zonula occludens-1 (ZO-1) tight junction protein was evaluated by using immunostaining at 24 and 48 hours after bEnd.3 cells were stimulated with LPS.

24 hours after bEnd.3 cells were stimulated with LPS, the total mean intensity of ZO-1 signal significantly decreased by 18 % when compared to the control cells, and glibenclamide was able to recover ZO-1 expression (Figure 3.7). Besides, control and LPS+Glib groups did not differ from each other significantly ($p = 0.9200$). In addition to the reduction in the protein expression of ZO-1, there were also prominent disruptions on the plasma membrane in cells that were exposed to LPS, and glibenclamide was able to restore the typical integrity of ZO-1 tight junction protein on the plasma membrane.

The total mean intensity of ZO-1 signal intensity remained the same among all groups (control, LPS, LPS+Glib) at 48 hours (Figure 3.8). However, the expression pattern of ZO-1 was discontinuous on the plasma membrane and was also detected within the cytoplasm in bEnd.3 cells exposed to LPS, and glibenclamide was able to restore the structural integrity of ZO-1 expression.

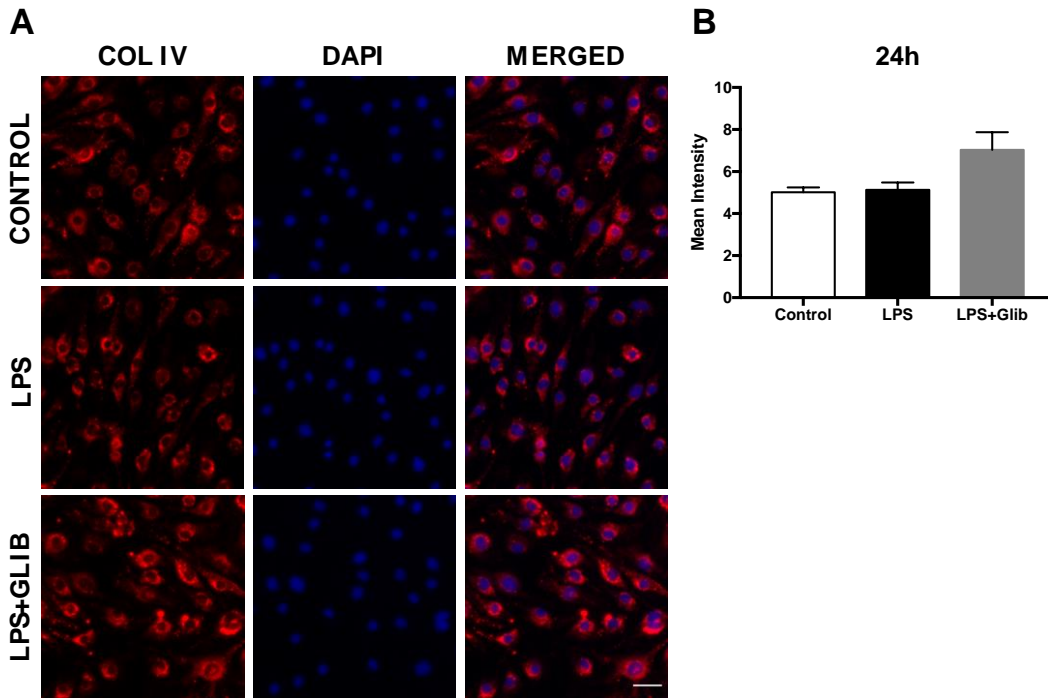


Figure 3.5. Glibenclamide interferes with collagen IV in 24 hours LPS stimulated bEnd.3 cells. A) Representative COL IV, DAPI and merged images are from control, LPS and LPS+Glib groups. B) Quantitative analysis of COL IV images is demonstrated for 24 hours LPS incubation. Results are given as mean \pm SEM; n=2. Scale Bar: 50 μ m.

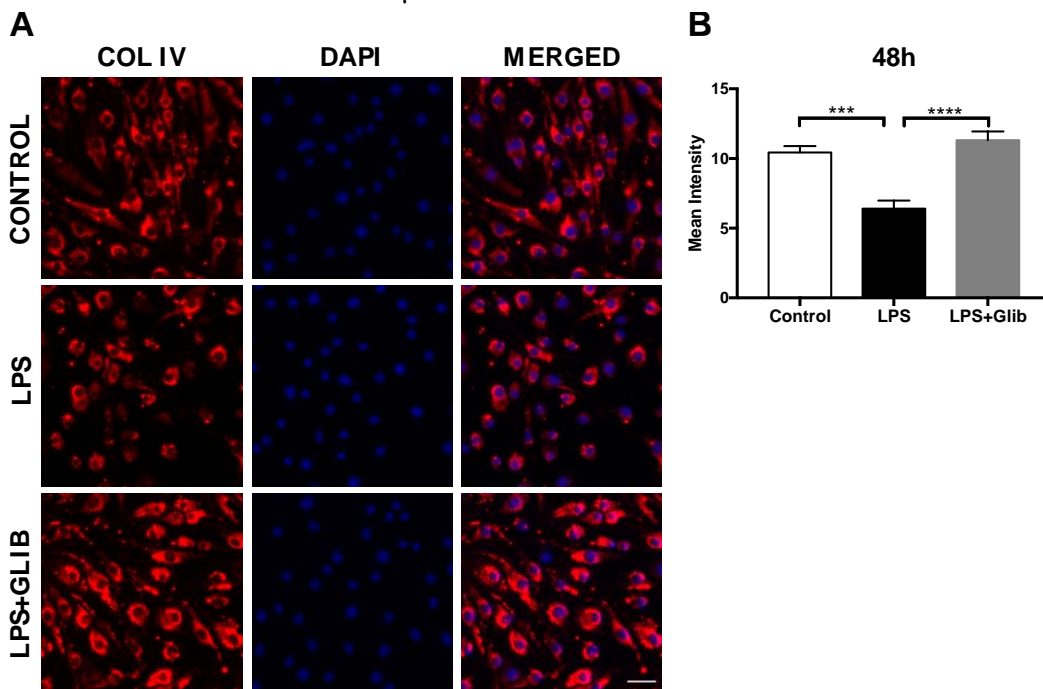


Figure 3.6. Glibenclamide increases the amount of collagen IV in 48 hours LPS stimulated bEnd.3 cells. A) Representative COL IV, DAPI and merged images are from control, LPS and LPS+Glib groups. B) Quantitative analysis of COL IV images is demonstrated for 48 hours LPS incubation. Results are given as mean \pm SEM. (***)p<0.001; (****)p<0.0001 Scale Bar: 50 μ m.

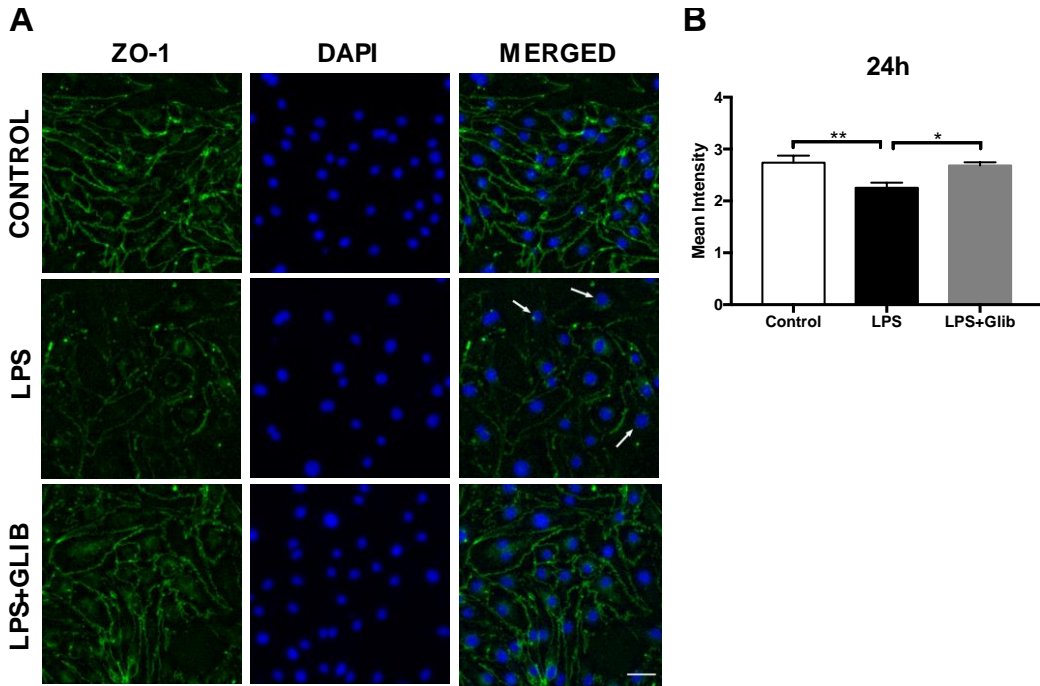


Figure 3.7. Glibenclamide restores the tight junction protein, zonula occludens-1 in 24 hours LPS stimulated bEnd.3 cells. A) Representative ZO-1, DAPI and merged images are from control, LPS and LPS+Glib groups. B) Quantitative analysis of ZO-1 demonstrated for 24 hours LPS incubation. Results are given as mean \pm SEM. (* $p < 0.05$; ** $p < 0.01$) Arrows show ZO-1 disruptions on the plasma membrane. Scale Bar: 50 μ m.

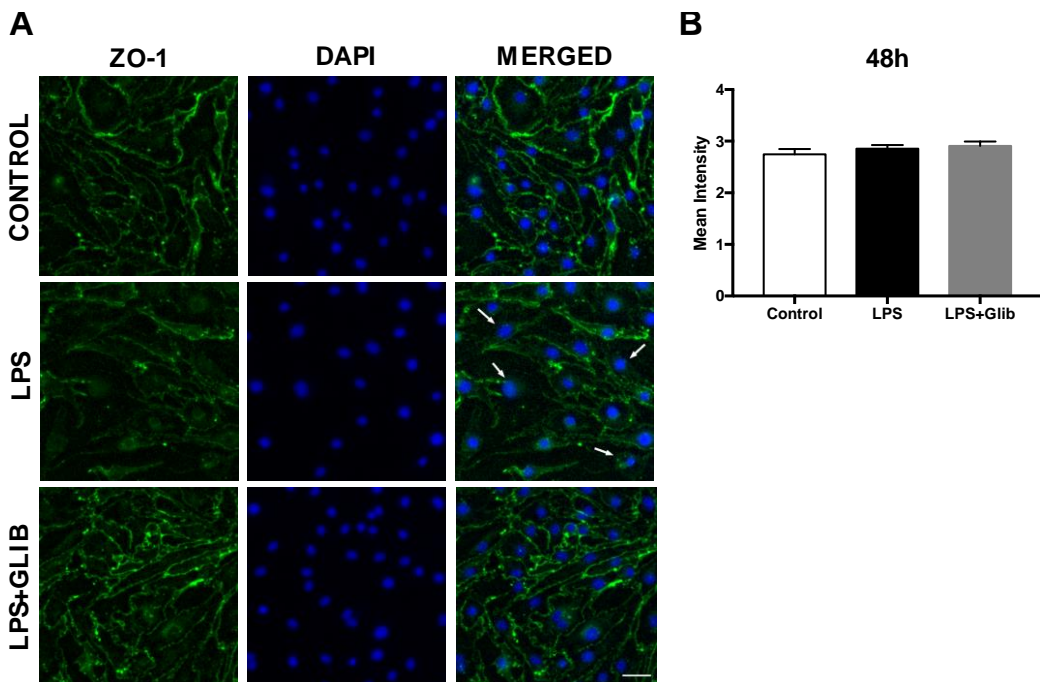


Figure 3.8. Glibenclamide restores the tight junction protein, zonula occludens-1 in 48 hour LPS stimulated bEnd.3 cells. A) Representative ZO-1, DAPI and merged images are from control, LPS and LPS+Glib groups. B) Quantitative analysis of ZO-1 images is demonstrated for 48 hours LPS incubation. Results are given as mean \pm SEM. Arrows show ZO-1 disruptions on the plasma membrane. Scale Bar: 50 μ m.

Furthermore, control and LPS+Glib group of cells predominantly appeared elongated in shape and similar in morphology, whereas cells exposed to LPS were mostly circular in shape at both time-points observed, which could be interpreted as cell retraction due to actin polymerization ^[72].

CHAPTER 4

DISCUSSION

TLR4 signaling plays a crucial role in the innate immune system and give inflammatory responses directed to destroy bacterial infections. Lately, the involvement of TLR4 signaling has been linked to stroke, TBI and Alzheimer's diseases [73-75]. Even though the exact mechanism of TLR4 is not known after stroke and TBI, it is thought that TLR4 signaling triggers neuroinflammation and has been linked to brain damage [73-74]. By taking these pathologies into consideration, understanding TLR4 signaling is important in order to reduce the inflammatory response, cell death and the associated brain damage.

LPS stimulated (neuro)inflammation has been well-studied both *in vitro* and *in vivo* and the molecular mechanism has been well-established [76-77]. LPS initiates a signaling cascade initially with the TLR4 receptor, which then causes the nuclear translocation of the transcription factor, NF κ B can then specifically upregulate several proinflammatory cytokines like TNF α , IL1- β and IL6, and activate caspase 1, caspase 3, caspase 6 and caspase 8 [47]. In addition, NF κ B can promote the expression and colocalization of Sur1 with Trpm4, due to the two consensus sequences for NF κ B found at the promoter region of the *Abcc8* gene [37]. Furthermore, it has previously been shown that Sur1 and Trpm4 colocalize with each other in neurons, astrocytes, endothelial and microglial cells both in animal models and patients after stroke and TBI by immunoprecipitation and FRET analysis [26-27, 78].

In this study, we took advantage of LPS to demonstrate the upregulation of Sur1-Trpm4 channels to mimic CNS pathologies *in vitro* by using brain microvascular endothelial cells. Moreover, we used glibenclamide as an antagonist of Sur1-Trpm4 channels to reduce the release of LPS stimulated proinflammatory cytokines, expression of Sur1-Trpm4 channels, cell death and eventually the disruption of the BBB and the associated structural proteins.

One of the hallmarks of LPS stimulation is the nuclear translocation of the transcription factor NF κ B. Endothelial cells express the TLR4 receptor, that convey the LPS signal with the help of the adaptor protein Myd88, which can then recruit protein

kinases IRAK1, and TRAF6 [49]. TRAF6 is able to activate IKK, which phosphorylates and targets I κ B for protein degradation via the ubiquitin proteasome pathway. After that, NF κ B is released from I κ B and can translocate into the nucleus. In our study, we demonstrated that 24 and 48 hours of LPS stimulation in bEnd.3 cells was sufficient to induce significant NF κ B translocation into the nucleus and glibenclamide was able to significantly attenuate this translocation and associated inflammatory response. To our knowledge, this study is the first to show the link between NF κ B and glibenclamide in LPS stimulated brain microvascular endothelial cells. It is important to note that glibenclamide is not a direct inhibitor of any protein within the NF κ B signaling pathway. LPS has been demonstrated to increase intracellular calcium levels, which can be inhibited by glibenclamide in microglial cells [24]. Furthermore, increased intracellular calcium can affect the Ca²⁺ dependent kinases, which are responsible for the induction of I κ B phosphorylation, leading to the nuclear translocalization of NF κ B [79-80]. Even though we did not check the intracellular calcium levels for this study, it is highly possible to think that glibenclamide can exert its anti-inflammatory effect by regulating intracellular calcium levels, which can then induce NF κ B translocation in LPS stimulated bEnd.3 cells. Additionally, the study of Pompenmayer *et al.* has revealed the protective effect of glibenclamide in the kidney model of ischemia/reperfusion injury [81]. The authors attributed the protective effect of glibenclamide to its ability to inhibit TNF α production, which further prevents NF κ B translocation in renal tissue. Similarly, it is plausible to think that glibenclamide can act as an anti-inflammatory agent in LPS stimulated brain endothelial cells by either reducing the expression or preventing the release of TNF α , ultimately hindering NF κ B nuclear translocation.

Exposure of endothelial cells to LPS has been linked to apoptotic cell death both *in vitro* and *in vivo* studies [82-83]. DNA fragmentation after LPS stimulation in bovine and sheep endothelial cells has been associated with apoptosis [69, 82]. Furthermore, intravenous and intraperitoneal LPS administration to rats showed elevated caspase-3 activity in the liver endothelial cells [83-84]. In our study, we also confirmed that LPS stimulation for 24 hours leads to caspase-3 dependent apoptotic cell death in bEnd.3 cells. Increased amounts of cleaved caspase-3 protein was demonstrated by both immunostaining and immunoblotting techniques. Elevated caspase-3 expression can be attributed to TNF α release following LPS exposure, which in turn can bind to TNF α receptor 1 (TNFR1) and recruit Fas associated death domain (FADD) [84]. FADD can also

bind to Myd88 and recruit procaspase-8^[48]. Eventually, activated procaspase-8 can cleave other caspases like procaspase-8 and procaspase-3 leading to the activation of cleaved caspase-3, the executioner^[47].

In addition to apoptosis, we demonstrated cell death in LPS stimulated bEnd.3 cells via PI and Hoechst staining. At both 24 and 48 hours after LPS induction, LPS increased the observed cell death with a significant increase in PI staining.

Upregulation of MMP2/9 causes BBB breakdown, vasogenic edema and eventually hemorrhagic transformation in stroke patients, which has been associated with high mortality and poor neurological outcomes^[85-86]. Additionally, there is a biphasic activation of MMP2 and MMP9, where the former one is involved more actively within the first hours of stroke and the latter one is more effective during 24-48 hours post stroke^[85]. As a result of translocation of transcriptional factors like NFκB, AP1 and SP1, prominently elevated expressions/activities of MMP2 and MMP9 has been widely reported in stroke and trauma patients^[37, 87]. Therefore, it is reasonable to think that the expressions/activities of MMP2/9 are inevitable results of LPS stimulation, that can result in the degradation of the basal lamina and tight junction proteins as their substrate. Based on our results, we observed a decreasing trend in the collagen IV protein level in bEnd.3 cells that do not reach significance at 24 hours after LPS stimulation. This reduction became significant at 48 hours after LPS stimulation, which can be attributed to the late activation of MMP9. Moreover, glibenclamide was able to recover the collagen IV expression in LPS stimulated bEnd.3 cells, which is consistent with the previous studies of Simard *et al.*, Sheth *et al* and Tosun *et al.* where authors demonstrated reduced expression/activity of MMP9 in brain endothelial cells, human stroke patients, and neonatal ischemic rats when they were treated with glibenclamide^[88-90].

ZO-1 protein is typically linked to the cytosolic actin and plays a critical role in the regulation of BBB integrity^[1]. Intracellular junctional localization of ZO-1 has been shown to be disrupted in endothelial cells following LPS exposure through actin polymerization^[43, 52]. In our immunostaining results, ZO-1 expression was significantly decreased at 24 hours after LPS stimulation in bEnd.3 cells. More importantly, its integrity was disrupted at both 24 and 48 hours following LPS exposure. Interestingly, the expressions of ZO-1 in all groups remained the same 48 hours after the addition of LPS, which can be explained by the alteration in the specific localization of ZO-1 protein without changing the total mean intensity signal. Furthermore, glibenclamide provided a partial recovery of ZO-1 in LPS stimulated bEnd.3 cells, which is consistent with the

study of Simard *et al.*, in which authors showed recovery of the BBB permeability and ZO-1 localization in glibenclamide treated rodent SAH model ^[43]. In addition, in the studies of Wojciak-Stothard *et al.* and Blum *et al.*, where inflammation in endothelial cells was induced with TNF α incubation, authors provided evidence in which the adverse effect of TNF α also caused the discontinuous distribution pattern of ZO-1 expression ^[91-92]. This also supports the idea that glibenclamide can possibly exert its protective effect through TNF α signaling.

CHAPTER 5

CONCLUSION

Activation of TLR signaling has been associated with both CNS injuries and associated neurologic disorders. That is why the understanding of TLR signaling pathways is critical in order to cope with these pathologies. Additionally, in several CNS injury models and patient studies, Sur1-Trpm4 channels have been reported to be upregulated, which has been correlated with the associated cell death. In this study, we took advantage of the presence of two consensus sequences in which NF- κ B can bind to the promoter region of *Abcc8* gene, which encodes Sur1 protein. We induced brain microvascular endothelial cells to LPS to initiate the TLR4 signaling cascade to mimic CNS pathologies *in vitro*. Once TLR4 signaling is initiated, NF- κ B can translocate into the nucleus, where it can upregulate Sur1-Trpm4 channels, proinflammatory cytokines and trigger cell death. Furthermore, we investigated the protective effect of glibenclamide, an inhibitor of the Sur1-Trpm4 channel, on LPS stimulated brain microvascular endothelial cells. Our results revealed that glibenclamide exerts a protective effect in LPS stimulated brain microvascular endothelial cells by significantly reducing cell death, NF- κ B translocation and the maintenance of key structural proteins (COL IV and ZO-1) that are essential for the BBB integrity. In conclusion, glibenclamide can be used as a therapeutic agent to attenuate LPS stimulated inflammation in brain microvascular endothelial cells.

REFERENCES

1. Persidsky, Y.; Ramirez, S. H.; Haorah, J.; Kanmogne, G. D., Blood-brain barrier: structural components and function under physiologic and pathologic conditions. *J Neuroimmune Pharmacol* **2006**, *1* (3), 223-36.
2. Abbott, N. J.; Ronnback, L.; Hansson, E., Astrocyte-endothelial interactions at the blood-brain barrier. *Nat Rev Neurosci* **2006**, *7* (1), 41-53.
3. Huber, J. D.; Egleton, R. D.; Davis, T. P., Molecular physiology and pathophysiology of tight junctions in the blood-brain barrier. *Trends Neurosci* **2001**, *24* (12), 719-25.
4. Desai, B. S.; Monahan, A. J.; Carvey, P. M.; Hendey, B., Blood-brain barrier pathology in Alzheimer's and Parkinson's disease: implications for drug therapy. *Cell Transplant* **2007**, *16* (3), 285-99.
5. Orihuela, C. J.; Mahdavi, J.; Thornton, J.; Mann, B.; Wooldridge, K. G.; Abouseada, N.; Oldfield, N. J.; Self, T.; Ala'Aldeen, D. A.; Tuomanen, E. I., Laminin receptor initiates bacterial contact with the blood brain barrier in experimental meningitis models. *J Clin Invest* **2009**, *119* (6), 1638-46.
6. Dallasta, L. M.; Pisarov, L. A.; Esplen, J. E.; Werley, J. V.; Moses, A. V.; Nelson, J. A.; Achim, C. L., Blood-brain barrier tight junction disruption in human immunodeficiency virus-1 encephalitis. *Am J Pathol* **1999**, *155* (6), 1915-27.
7. Kirk, J.; Plumb, J.; Mirakhur, M.; McQuaid, S., Tight junctional abnormality in multiple sclerosis white matter affects all calibres of vessel and is associated with blood-brain barrier leakage and active demyelination. *J Pathol* **2003**, *201* (2), 319-27.
8. Yang, Y.; Rosenberg, G. A., Blood-brain barrier breakdown in acute and chronic cerebrovascular disease. *Stroke* **2011**, *42* (11), 3323-8.
9. Barzo, P.; Marmarou, A.; Fatouros, P.; Corwin, F.; Dunbar, J., Magnetic resonance imaging-monitored acute blood-brain barrier changes in experimental traumatic brain injury. *J Neurosurg* **1996**, *85* (6), 1113-21.

10. Stokum, J. A.; Gerzanich, V.; Simard, J. M., Molecular pathophysiology of cerebral edema. *J Cereb Blood Flow Metab* **2016**, *36* (3), 513-38.
11. Hawkins, B. T.; Davis, T. P., The blood-brain barrier/neurovascular unit in health and disease. *Pharmacol Rev* **2005**, *57* (2), 173-85.
12. Heo, J. H.; Lucero, J.; Abumiya, T.; Koziol, J. A.; Copeland, B. R.; del Zoppo, G. J., Matrix metalloproteinases increase very early during experimental focal cerebral ischemia. *J Cereb Blood Flow Metab* **1999**, *19* (6), 624-33.
13. Heo, J. H.; Lucero, J.; Abumiya, T.; Koziol, J. A.; Copeland, B. R.; del Zoppo, G. J., Matrix metalloproteinases increase very early during experimental focal cerebral ischemia. *J Cerebr Blood F Met* **1999**, *19* (6), 624-633.
14. Asahi, M.; Asahi, K.; Jung, J. C.; del Zoppo, G. J.; Fini, M. E.; Lo, E. H., Role for matrix metalloproteinase 9 after focal cerebral ischemia: effects of gene knockout and enzyme inhibition with BB-94. *J Cereb Blood Flow Metab* **2000**, *20* (12), 1681-9.
15. Wang, J.; Tsirka, S. E., Neuroprotection by inhibition of matrix metalloproteinases in a mouse model of intracerebral haemorrhage. *Brain* **2005**, *128* (Pt 7), 1622-33.
16. Feiler, S.; Plesnila, N.; Thal, S. C.; Zausinger, S.; Scholler, K., Contribution of matrix metalloproteinase-9 to cerebral edema and functional outcome following experimental subarachnoid hemorrhage. *Cerebrovasc Dis* **2011**, *32* (3), 289-95.
17. Aguilar-Bryan, L.; Nichols, C. G.; Wechsler, S. W.; Clement, J. P. t.; Boyd, A. E., 3rd; Gonzalez, G.; Herrera-Sosa, H.; Nguy, K.; Bryan, J.; Nelson, D. A., Cloning of the beta cell high-affinity sulfonylurea receptor: a regulator of insulin secretion. *Science* **1995**, *268* (5209), 423-6.
18. Simard, J. M.; Sheth, K. N.; Kimberly, W. T.; Stern, B. J.; del Zoppo, G. J.; Jacobson, S.; Gerzanich, V., Glibenclamide in cerebral ischemia and stroke. *Neurocrit Care* **2014**, *20* (2), 319-33.
19. Bataille, D., [Molecular mechanisms of insulin secretion]. *Diabetes Metab* **2002**, *28* (6 Suppl), 4S7-13.

20. Olokoba, A. B.; Obateru, O. A.; Olokoba, L. B., Type 2 diabetes mellitus: a review of current trends. *Oman Med J* **2012**, *27* (4), 269-73.
21. Intensive blood-glucose control with sulphonylureas or insulin compared with conventional treatment and risk of complications in patients with type 2 diabetes (UKPDS 33). UK Prospective Diabetes Study (UKPDS) Group. *Lancet* **1998**, *352* (9131), 837-53.
22. Castro, L.; Noelia, M.; Vidal-Jorge, M.; Sanchez-Ortiz, D.; Gandara, D.; Martinez-Saez, E.; Cicuendez, M.; Poca, M. A.; Simard, J. M.; Sahuquillo, J., Kir6.2, the Pore-Forming Subunit of ATP-Sensitive K(+) Channels, Is Overexpressed in Human Posttraumatic Brain Contusions. *J Neurotrauma* **2018**.
23. Ortega, F. J.; Gimeno-Bayon, J.; Espinosa-Parrilla, J. F.; Carrasco, J. L.; Batlle, M.; Pugliese, M.; Mahy, N.; Rodriguez, M. J., ATP-dependent potassium channel blockade strengthens microglial neuroprotection after hypoxia-ischemia in rats. *Exp Neurol* **2012**, *235* (1), 282-96.
24. Kurland, D. B.; Gerzanich, V.; Karimy, J. K.; Woo, S. K.; Vennekens, R.; Freichel, M.; Nilius, B.; Bryan, J.; Simard, J. M., The Sur1-Trpm4 channel regulates NOS2 transcription in TLR4-activated microglia. *J Neuroinflamm* **2016**, *13*.
25. Chen, M. K.; Dong, Y. F.; Simard, J. M., Functional coupling between sulfonylurea receptor type 1 and a nonselective cation channel in reactive astrocytes from adult rat brain. *Journal of Neuroscience* **2003**, *23* (24), 8568-8577.
26. Simard, J. M.; Chen, M.; Tarasov, K. V.; Bhatta, S.; Ivanova, S.; Melnitchenko, L.; Tsybalyuk, N.; West, G. A.; Gerzanich, V., Newly expressed SUR1-regulated NC(Ca-ATP) channel mediates cerebral edema after ischemic stroke. *Nat Med* **2006**, *12* (4), 433-40.
27. Mehta, R. I.; Tosun, C.; Ivanova, S.; Tsybalyuk, N.; Famakin, B. M.; Kwon, M. S.; Castellani, R. J.; Gerzanich, V.; Simard, J. M., Sur1-Trpm4 Cation Channel Expression in Human Cerebral Infarcts. *J Neuropath Exp Neur* **2015**, *74* (8), 835-849.
28. Tosun, C.; Kurland, D. B.; Mehta, R.; Castellani, R. J.; deJong, J. L.; Kwon, M. S.; Woo, S. K.; Gerzanich, V.; Simard, J. M., Inhibition of the Sur1-Trpm4 channel reduces neuroinflammation and cognitive impairment in subarachnoid hemorrhage. *Stroke* **2013**, *44* (12), 3522-8.

29. Lee, J. Y.; Choi, H. Y.; Na, W. H.; Ju, B. G.; Yune, T. Y., Ghrelin inhibits BSCB disruption/hemorrhage by attenuating MMP-9 and SUR1/TrpM4 expression and activation after spinal cord injury. *Biochim Biophys Acta* **2014**, *1842* (12 Pt A), 2403-12.
30. Makar, T. K.; Gerzanich, V.; Nimmagadda, V. K.; Jain, R.; Lam, K.; Mubariz, F.; Trisler, D.; Ivanova, S.; Woo, S. K.; Kwon, M. S.; Bryan, J.; Bever, C. T.; Simard, J. M., Silencing of Abcc8 or inhibition of newly upregulated Sur1-Trpm4 reduce inflammation and disease progression in experimental autoimmune encephalomyelitis. *J Neuroinflammation* **2015**, *12*, 210.
31. Martinez-Valverde, T.; Vidal-Jorge, M.; Martinez-Saez, E.; Castro, L.; Arikan, F.; Cordero, E.; Radoi, A.; Poca, M. A.; Simard, J. M.; Sahuquillo, J., Sulfonylurea Receptor 1 in Humans with Post-Traumatic Brain Contusions. *J Neurotrauma* **2015**, *32* (19), 1478-87.
32. Simard, J. M.; Kilbourne, M.; Tsybalyuk, O.; Tosun, C.; Caridi, J.; Ivanova, S.; Keledjian, K.; Bochicchio, G.; Gerzanich, V., Key role of sulfonylurea receptor 1 in progressive secondary hemorrhage after brain contusion. *J Neurotrauma* **2009**, *26* (12), 2257-67.
33. Jiang, B.; Li, L.; Chen, Q.; Tao, Y.; Yang, L.; Zhang, B.; Zhang, J. H.; Feng, H.; Chen, Z.; Tang, J.; Zhu, G., Role of Glibenclamide in Brain Injury After Intracerebral Hemorrhage. *Transl Stroke Res* **2017**, *8* (2), 183-193.
34. Zhou, F. F.; Liu, Y. J.; Yang, B. B.; Hu, Z. P., Neuroprotective potential of glibenclamide is mediated by antioxidant and anti-apoptotic pathways in intracerebral hemorrhage. *Brain Res Bull* **2018**, *142*, 18-24.
35. Tosun, C.; Koltz, M. T.; Kurland, D. B.; Ijaz, H.; Gurakar, M.; Schwartzbauer, G.; Coksaygan, T.; Ivanova, S.; Gerzanich, V.; Simard, J. M., The protective effect of glibenclamide in a model of hemorrhagic encephalopathy of prematurity. *Brain Sci* **2013**, *3* (1), 215-38.
36. Kahle, K. T.; Simard, J. M.; Staley, K. J.; Nahed, B. V.; Jones, P. S.; Sun, D. D., Molecular Mechanisms of Ischemic Cerebral Edema: Role of Electroneutral Ion Transport. *Physiology* **2009**, *24* (4), 257-265.

37. Simard, J. M.; Kent, T. A.; Chen, M.; Tarasov, K. V.; Gerzanich, V., Brain oedema in focal ischaemia: molecular pathophysiology and theoretical implications. *Lancet Neurol* **2007**, *6* (3), 258-68.
38. Simard, J. M.; Tarasov, K. V.; Gerzanich, V., Non-selective cation channels, transient receptor potential channels and ischemic stroke. *Biochim Biophys Acta* **2007**, *1772* (8), 947-57.
39. Woo, S. K.; Kwon, M. S.; Geng, Z.; Chen, Z.; Ivanov, A.; Bhatta, S.; Gerzanich, V.; Simard, J. M., Sequential activation of hypoxia-inducible factor 1 and specificity protein 1 is required for hypoxia-induced transcriptional stimulation of Abcc8. *J Cereb Blood Flow Metab* **2012**, *32* (3), 525-36.
40. Kunte, H.; Schmidt, S.; Eliasziw, M.; del Zoppo, G. J.; Simard, J. M.; Masuhr, F.; Weih, M.; Dirnagl, U., Sulfonylureas improve outcome in patients with type 2 diabetes and acute ischemic stroke. *Stroke* **2007**, *38* (9), 2526-30.
41. Wali, B.; Ishrat, T.; Atif, F.; Hua, F.; Stein, D. G.; Sayeed, I., Glibenclamide Administration Attenuates Infarct Volume, Hemispheric Swelling, and Functional Impairments following Permanent Focal Cerebral Ischemia in Rats. *Stroke Res Treat* **2012**, *2012*, 460909.
42. Simard, J. M.; Yurovsky, V.; Tsymbalyuk, N.; Melnichenko, L.; Ivanova, S.; Gerzanich, V., Protective effect of delayed treatment with low-dose glibenclamide in three models of ischemic stroke. *Stroke* **2009**, *40* (2), 604-9.
43. Simard, J. M.; Geng, Z.; Woo, S. K.; Ivanova, S.; Tosun, C.; Melnichenko, L.; Gerzanich, V., Glibenclamide reduces inflammation, vasogenic edema, and caspase-3 activation after subarachnoid hemorrhage. *J Cereb Blood Flow Metab* **2009**, *29* (2), 317-30.
44. Simard, J. M.; Tsymbalyuk, O.; Ivanov, A.; Ivanova, S.; Bhatta, S.; Geng, Z.; Woo, S. K.; Gerzanich, V., Endothelial sulfonylurea receptor 1-regulated NC Ca-ATP channels mediate progressive hemorrhagic necrosis following spinal cord injury. *J Clin Invest* **2007**, *117* (8), 2105-13.
45. Gardiner, S. M.; Kemp, P. A.; March, J. E.; Bennett, T., Regional haemodynamic responses to infusion of lipopolysaccharide in conscious rats: effects of pre- or post-treatment with glibenclamide. *Br J Pharmacol* **1999**, *128* (8), 1772-8.

46. Wu, C. C.; Thiernemann, C.; Vane, J. R., Glibenclamide-induced inhibition of the expression of inducible nitric oxide synthase in cultured macrophages and in the anaesthetized rat. *Br J Pharmacol* **1995**, *114* (6), 1273-81.
47. Bannerman, D. D.; Goldblum, S. E., Mechanisms of bacterial lipopolysaccharide-induced endothelial apoptosis. *Am J Physiol Lung Cell Mol Physiol* **2003**, *284* (6), L899-914.
48. Dauphinee, S. M.; Karsan, A., Lipopolysaccharide signaling in endothelial cells. *Lab Invest* **2006**, *86* (1), 9-22.
49. Akira, S.; Takeda, K., Toll-like receptor signalling. *Nature Reviews Immunology* **2004**, *4* (7), 499-511.
50. Mukherjee, S.; Huda, S.; Sinha Babu, S. P., Toll-like receptor polymorphism in host immune response to infectious diseases: A review. *Scand J Immunol* **2019**, e12771.
51. Magrone, T.; Jirillo, E., The impact of bacterial lipopolysaccharides on the endothelial system: pathological consequences and therapeutic countermeasures. *Endocr Metab Immune Disord Drug Targets* **2011**, *11* (4), 310-25.
52. Bierhaus, A.; Chen, J.; Liliensiek, B.; Nawroth, P. P., LPS and cytokine-activated endothelium. *Semin Thromb Hemost* **2000**, *26* (5), 571-87.
53. Lichtman, S. N.; Wang, J.; Lemasters, J. J., Lipopolysaccharide-stimulated TNF- α release from cultured rat Kupffer cells: sequence of intracellular signaling pathways. *J Leukocyte Biol* **1998**, *64* (3), 368-372.
54. Buchanan, M. M.; Hutchinson, M.; Watkins, L. R.; Yin, H., Toll-like receptor 4 in CNS pathologies. *J Neurochem* **2010**, *114* (1), 13-27.
55. Plociennikowska, A.; Hromada-Judycka, A.; Borzecka, K.; Kwiatkowska, K., Co-operation of TLR4 and raft proteins in LPS-induced pro-inflammatory signaling. *Cell Mol Life Sci* **2015**, *72* (3), 557-581.
56. Lehnardt, S.; Lachance, C.; Patrizi, S.; Lefebvre, S.; Follett, P. L.; Jensen, F. E.; Rosenberg, P. A.; Volpe, J. J.; Vartanian, T., The toll-like receptor TLR4 is necessary for lipopolysaccharide-induced oligodendrocyte injury in the CNS. *J Neurosci* **2002**, *22* (7), 2478-86.

57. Lively, S.; Schlichter, L. C., Microglia Responses to Pro-inflammatory Stimuli (LPS, IFN γ +TNF α) and Reprogramming by Resolving Cytokines (IL-4, IL-10). *Front Cell Neurosci* **2018**, *12*, 215.
58. Zeuke, S.; Ulmer, A. J.; Kusumoto, S.; Katus, H. A.; Heine, H., TLR4-mediated inflammatory activation of human coronary artery endothelial cells by LPS. *Cardiovasc Res* **2002**, *56* (1), 126-34.
59. Schroder, J. M.; Christophers, E., Secretion of novel and homologous neutrophil-activating peptides by LPS-stimulated human endothelial cells. *J Immunol* **1989**, *142* (1), 244-51.
60. Bogatcheva, N. V.; Zemskova, M. A.; Kovalenkov, Y.; Poirier, C.; Verin, A. D., Molecular mechanisms mediating protective effect of cAMP on lipopolysaccharide (LPS)-induced human lung microvascular endothelial cells (HLMVEC) hyperpermeability. *J Cell Physiol* **2009**, *221* (3), 750-9.
61. Slivka, P. F.; Shridhar, M.; Lee, G. I.; Sammond, D. W.; Hutchinson, M. R.; Martinko, A. J.; Buchanan, M. M.; Sholar, P. W.; Kearney, J. J.; Harrison, J. A.; Watkins, L. R.; Yin, H., A peptide antagonist of the TLR4-MD2 interaction. *Chembiochem* **2009**, *10* (4), 645-9.
62. Kawai, T.; Takeuchi, O.; Fujita, T.; Inoue, J.; Muhlradt, P. F.; Sato, S.; Hoshino, K.; Akira, S., Lipopolysaccharide stimulates the MyD88-independent pathway and results in activation of IFN-regulatory factor 3 and the expression of a subset of lipopolysaccharide-inducible genes. *J Immunol* **2001**, *167* (10), 5887-94.
63. Olsen, K. M.; Kearns, G. L.; Kemp, S. F., Glyburide protein binding and the effect of albumin glycation in children, young adults, and older adults with diabetes. *J Clin Pharmacol* **1995**, *35* (7), 739-45.
64. Hemeda, H.; Giebel, B.; Wagner, W., Evaluation of human platelet lysate versus fetal bovine serum for culture of mesenchymal stromal cells. *Cytotherapy* **2014**, *16* (2), 170-80.
65. Koide, N.; Abe, K.; Narita, K.; Kato, Y.; Sugiyama, T.; Jiang, G. Z.; Yokochi, T., Apoptotic cell death of vascular endothelial cells and renal tubular cells in the generalized Shwartzman reaction. *FEMS Immunol Med Microbiol* **1996**, *16* (3-4), 205-11.

66. Zhang, C. Y.; Huang, J.; Kang, X. T., Resveratrol Attenuates LPS-induced Apoptosis via Inhibiting NF-kappa B Activity in Chicken Peripheral Lymphocyte Cultures. *Braz J Poultry Sci* **2018**, *20* (4), 747-752.
67. Xaus, J.; Comalada, M.; Valledor, A. F.; Lloberas, J.; Lopez-Soriano, F.; Argiles, J. M.; Bogdan, C.; Celada, A., LPS induces apoptosis in macrophages mostly through the autocrine production of TNF-alpha. *Blood* **2000**, *95* (12), 3823-3831.
68. Choi, K. B.; Wong, F.; Harlan, J. M.; Chaudhary, P. M.; Hood, L.; Karsan, A., Lipopolysaccharide mediates endothelial apoptosis by a FADD-dependent pathway. *J Biol Chem* **1998**, *273* (32), 20185-20188.
69. Hoyt, D. G.; Mannix, R. J.; Gerritsen, M. E.; Watkins, S. C.; Lazo, J. S.; Pitt, B. R., Integrins inhibit LPS-induced DNA strand breakage in cultured lung endothelial cells. *Am J Physiol-Lung C* **1996**, *270* (4), L689-L694.
70. Messner, U. K.; Briner, V. A.; Pfeilschifter, J., Tumor necrosis factor-alpha and lipopolysaccharide induce apoptotic cell death in bovine glomerular endothelial cells. *Kidney International* **1999**, *55* (6), 2322-2337.
71. Munshi, N.; Fernandis, A. Z.; Cherla, R. P.; Park, I. W.; Ganju, R. K., Lipopolysaccharide-induced apoptosis of endothelial cells and its inhibition by vascular endothelial growth factor. *J Immunol* **2002**, *168* (11), 5860-5866.
72. Prasain, N.; Stevens, T., The actin cytoskeleton in endothelial cell phenotypes. *Microvascular Research* **2009**, *77* (1), 53-63.
73. Caso, J. R.; Pradillo, J. M.; Hurtado, O.; Lorenzo, P.; Moro, M. A.; Lizasoain, I., Toll-like receptor 4 is involved in brain damage and inflammation after experimental stroke. *Circulation* **2007**, *115* (12), 1599-608.
74. Zhu, H. T.; Bian, C.; Yuan, J. C.; Chu, W. H.; Xiang, X.; Chen, F.; Wang, C. S.; Feng, H.; Lin, J. K., Curcumin attenuates acute inflammatory injury by inhibiting the TLR4/MyD88/NF-kappaB signaling pathway in experimental traumatic brain injury. *J Neuroinflammation* **2014**, *11*, 59.
75. Sheng, J. G.; Bora, S. H.; Xu, G.; Borchelt, D. R.; Price, D. L.; Koliatsos, V. E., Lipopolysaccharide-induced-neuroinflammation increases intracellular accumulation of amyloid precursor protein and amyloid beta peptide in APP^{swe} transgenic mice. *Neurobiol Dis* **2003**, *14* (1), 133-45.

76. Kawai, T.; Akira, S., The role of pattern-recognition receptors in innate immunity: update on Toll-like receptors. *Nat Immunol* **2010**, *11* (5), 373-84.
77. Nagai, Y.; Akashi, S.; Nagafuku, M.; Ogata, M.; Iwakura, Y.; Akira, S.; Kitamura, T.; Kosugi, A.; Kimoto, M.; Miyake, K., Essential role of MD-2 in LPS responsiveness and TLR4 distribution. *Nat Immunol* **2002**, *3* (7), 667-72.
78. Gerzanich, V.; Stokum, J. A.; Ivanova, S.; Woo, S. K.; Tsybalyuk, O.; Sharma, A.; Akkenti, F.; Imran, Z.; Aarabi, B.; Sahuquillo, J.; Simard, J. M., Sulfonylurea Receptor 1, Transient Receptor Potential Cation Channel Subfamily M Member 4, and KIR6.2: Role in Hemorrhagic Progression of Contusion. *J Neurotrauma* **2019**, *36* (7), 1060-1079.
79. Khalaf, H.; Jass, J.; Olsson, P. E., The role of calcium, NF-kappaB and NFAT in the regulation of CXCL8 and IL-6 expression in Jurkat T-cells. *Int J Biochem Mol Biol* **2013**, *4* (3), 150-6.
80. Tabary, O.; Boncoeur, E.; de Martin, R.; Pepperkok, R.; Clement, A.; Schultz, C.; Jacquot, J., Calcium-dependent regulation of NF-B-kappa activation in cystic fibrosis airway epithelial cells. *Cellular Signalling* **2006**, *18* (5), 652-660.
81. Pompermayer, K.; Souza, D. G.; Lara, G. G.; Silveira, K. D.; Cassali, G. D.; Andrade, A. A.; Bonjardim, C. A.; Passaglio, K. T.; Assreuy, J.; Cunha, F. Q.; Vieira, M. A.; Teixeira, M. M., The ATP-sensitive potassium channel blocker glibenclamide prevents renal ischemia/reperfusion injury in rats. *Kidney Int* **2005**, *67* (5), 1785-96.
82. Frey, E. A.; Finlay, B. B., Lipopolysaccharide induces apoptosis in a bovine endothelial cell line via a soluble CD14 dependent pathway. *Microb Pathogenesis* **1998**, *24* (2), 101-109.
83. Deaciuc, I. V.; Fortunato, F.; D'Souza, N. B.; Hill, D. B.; Schmidt, J.; Lee, E. Y.; McClain, C. J., Modulation of caspase-3 activity and fas ligand mRNA expression in rat liver cells in vivo by alcohol and lipopolysaccharide. *Alcohol Clin Exp Res* **1999**, *23* (2), 349-356.
84. Wang, Y. J.; Singh, R.; Lefkowitz, J. H.; Rigoli, R. M.; Czaja, M. J., Tumor necrosis factor-induced toxic liver injury results from JNK2-dependent activation of caspase-8 and the mitochondrial death pathway. *J Biol Chem* **2006**, *281* (22), 15258-15267.

85. Turner, R. J.; Sharp, F. R., Implications of MMP9 for Blood Brain Barrier Disruption and Hemorrhagic Transformation Following Ischemic Stroke. *Front Cell Neurosci* **2016**, *10*, 56.
86. Pagenstecher, A.; Stalder, A. K.; Kincaid, C. L.; Volk, B.; Campbell, I. L., Regulation of matrix metalloproteinases and their inhibitor genes in lipopolysaccharide-induced endotoxemia in mice. *Am J Pathol* **2000**, *157* (1), 197-210.
87. Li, H.; Xu, H.; Sun, B., Lipopolysaccharide regulates MMP-9 expression through TLR4/NF-kappaB signaling in human arterial smooth muscle cells. *Mol Med Rep* **2012**, *6* (4), 774-8.
88. Kimberly, W. T.; Battey, T. W.; Pham, L.; Wu, O.; Yoo, A. J.; Furie, K. L.; Singhal, A. B.; Elm, J. J.; Stern, B. J.; Sheth, K. N., Glyburide is associated with attenuated vasogenic edema in stroke patients. *Neurocrit Care* **2014**, *20* (2), 193-201.
89. Gerzanich, V.; Kwon, M. S.; Woo, S. K.; Ivanov, A.; Simard, J. M., SUR1-TRPM4 channel activation and phasic secretion of MMP-9 induced by tPA in brain endothelial cells. *PLoS One* **2018**, *13* (4), e0195526.
90. Tosun, C.; Hong, C.; Carusillo, B.; Ivanova, S.; Gerzanich, V.; Simard, J. M., Angiogenesis induced by prenatal ischemia predisposes to periventricular hemorrhage during postnatal mechanical ventilation. *Pediatr Res* **2015**, *77* (5), 663-73.
91. Wojciak-Stothard, B.; Entwistle, A.; Garg, R.; Ridley, A. J., Regulation of TNF-alpha-induced reorganization of the actin cytoskeleton and cell-cell junctions by Rho, Rac, and Cdc42 in human endothelial cells. *J Cell Physiol* **1998**, *176* (1), 150-65.
92. Blum, M. S.; Toninelli, E.; Anderson, J. M.; Balda, M. S.; Zhou, J.; O'Donnell, L.; Pardi, R.; Bender, J. R., Cytoskeletal rearrangement mediates human microvascular endothelial tight junction modulation by cytokines. *Am J Physiol* **1997**, *273* (1 Pt 2), H286-94.